

**NICKEL HEAVY METAL AND DYE REMOVAL
USING POLYETHERSULFONE
MICROCAPSULE**

LEE YU SIN

UNIVERSITI TUNKU ABDUL RAHMAN

**NICKEL HEAVY METAL AND DYE REMOVAL USING
POLYETHERSULFONE MICROCAPSULE**

LEE YU SIN

**A project report submitted in partial fulfilment of the
requirements for the award of Bachelor of Chemical
Engineering with Honours**

**Lee Kong Chian Faculty of Engineering and Science
Universiti Tunku Abdul Rahman**

May 2024

DECLARATION

I hereby declare that this project report is based on my original work except for citations and quotations which have been duly acknowledged. I also declare that it has not been previously and concurrently submitted for any other degree or award at UTAR or other institutions.

Signature : Lee

Name : Lee Yu Sin


ID No. : 20UEB02905

Date : 16 May 2024

APPROVAL FOR SUBMISSION

I certify that this project report entitled “**NICKEL HEAVY METAL AND DYE REMOVAL USING POLYETHERSULFONE MICROCAPSULE**” was prepared by **LEE YU SIN** has met the required standard for submission in partial fulfilment of the requirements for the award of Bachelor of Chemical Engineering with Honours at Universiti Tunku Abdul Rahman.

Approved by,

Signature : 

Supervisor : Ts. Dr. Shuit Siew Hoong

Date : 16 May 2024

The copyright of this report belongs to the author under the terms of the copyright Act 1987 as qualified by Intellectual Property Policy of Universiti Tunku Abdul Rahman. Due acknowledgement shall always be made of the use of any material contained in, or derived from, this report.

© 2024, Lee Yu Sin. All right reserved.

ACKNOWLEDGEMENTS

I would like to thank everyone who had contributed to the successful completion of this project. I would like to express my gratitude to my research supervisor, Ts. Dr. Shuit Siew Hoong for his invaluable advice, guidance and his enormous patience throughout the development of the research.

In addition, I would also like to express my gratitude to my loving parents and family members who had helped and given me encouragement and support during my hardest times in the completion of final year project. Moreover, I would like to thank my friends who had given me advice and suggestions during my research and laboratory sessions.

ABSTRACT

The rapid growth of the global population and industrialization has led to increased discharge of organic and inorganic pollutants into water bodies. The wastewater needs to be treated, as it can bring adverse effects to human health. Conventional techniques for removing heavy metals and dyes from wastewater are costly and result in large amounts of sludge. Adsorption is considered as the most efficient wastewater treatment technology due to its reversibility and reusability of adsorbents. Therefore, PES microcapsule have the potential to remove of nickel (Ni) and methylene blue (MB) dye from the water. PES microspheres were synthesized using phase inversion method. Characterization results, such as scanning electron microscopy (SEM), revealed the porous structure of the microcapsules, while Fourier-transform infrared (FTIR) analysis verified the presence of the PES polymer. Thermogravimetric analysis (TGA) demonstrated the outstanding thermal stability of the PES microspheres. The Brunauer-Emmett-Teller (BET) specific surface area of the microcapsules was measured at $10.97 \text{ m}^2/\text{g}$. Furthermore, the pH drift method proved the presence of a negative charge on the surface of the microcapsules, which can facilitate the removal of cationic pollutants. Response surface methodology based on central composite design (CCD) was used to optimize the effects of different adsorption process parameters such as the pH (4 to 12), microcapsule loading (20 g/L to 40 g/L), and initial concentration (5 mg/L to 25 mg/L for Ni and 1 mg/L to 5 mg/L for MB dye). The optimum Ni removal efficiency was 94.92 % at a pH of 9.98, microcapsule loading of 25.16 g/L and initial concentration of nickel of 20.00 mg/L. Meanwhile, the optimum MB dye removal efficiency was 94.97 % at a pH of 11.99, microcapsule loading of 33.00 g/L and initial concentration of MB of 2.41 mg/L. It was discovered that pH had the highest impact on the removal efficiency, in which it could be improved by increasing the pH of the solution. The presence of Ni and MB dye in the pores of PES microcapsules has demonstrated that the successful adsorption of PES microcapsules was attributed to electrostatic interactions. It can be concluded that PES microspheres are promising adsorbent for removing Ni and MB dye from aqueous solutions, as they exhibited high removal efficiency.

TABLE OF CONTENTS

DECLARATION		i
APPROVAL FOR SUBMISSION		ii
ACKNOWLEDGEMENTS		iv
ABSTRACT		v
TABLE OF CONTENTS		vi
LIST OF TABLES		ix
LIST OF FIGURES		xi
LIST OF SYMBOLS / ABBREVIATIONS		xiii
LIST OF APPENDICES		xv
CHAPTER		
1	INTRODUCTION	16
1.1	General Introduction	16
1.2	Importance of the Study	19
1.3	Problem Statement	20
1.4	Aim and Objectives	21
1.5	Scope and Limitation of the Study	22
2	LITERATURE REVIEW	23
2.1	Heavy Metal	23
2.1.1	Sources and Emissions of Heavy Metal	23
2.1.2	Toxicity and Health Impact of Heavy Metals	24
2.2	Dyes	25
2.2.1	Sources and Emissions of Dyes	25
2.2.2	Toxicity and Health Impact of Dyes	26
2.3	Removal Techniques	26
2.3.1	Biological Techniques	27
2.3.2	Chemical Techniques	28
2.3.3	Physical Techniques	29

2.4	Adsorption Technology	30
2.4.1	Adsorption Mechanism	31
2.4.2	Types of Adsorbents	32
2.5	Polymer Microcapsule	35
2.5.1	PES microcapsule	35
2.6	Phase Inversion Method	36
2.7	Characterization Studies of PES Microcapsule	37
2.7.1	pH drift method	38
2.7.2	SEM-EDX	38
2.7.3	FTIR	41
2.7.4	BET	42
2.7.5	TGA	43
2.8	Effects of Process Parameters	43
2.8.1	Effect of pH	43
2.8.2	Effect of Microcapsule Loading	44
2.8.3	Effect of Initial Concentration	45
2.9	Response Surface Methodology (RSM)	47
3	METHODOLOGY AND WORK PLAN	49
3.1	Introduction	49
3.2	Materials and Chemicals	50
3.3	Equipment	51
3.4	Overall Process Flow Chart	52
3.5	Synthesis of PES Microcapsules	53
3.6	Characterization of PES microcapsules	53
3.6.1	SEM-EDX	53
3.6.2	BET	54
3.6.3	FTIR	54
3.6.4	TGA	54
3.6.5	pH drift	54
3.6	Preparation of Ni Stock Solution and MB Stock Solution	55
3.7	Design of Experiment Using Response Surface Methodology	55
3.8	Results Analysis	60

4	RESULTS AND DISCUSSION	61
4.1	Characterization Studies of PES Microcapsule	61
4.1.1	SEM-EDX	61
4.1.2	FTIR	66
4.1.3	Surface Area Analysis: BET Analysis	67
4.1.4	TGA	68
4.1.5	pH drift	70
4.2	Statistical Analysis and Optimization Design	
	Study of Ni Removal Efficiency	71
4.2.1	Regression Analysis of Ni Removal	71
4.2.2	Effect of Process Parameters on Ni Removal Efficiency	78
4.2.3	Optimization and Model Validation	85
4.3	Statistical Analysis and Optimization Design	
	Study of MB Removal Efficiency	87
4.3.1	Regression Analysis of MB Removal	87
4.3.2	Effect of Process Parameters on MB Removal	93
4.3.3	Optimization and Model Validation	98
4.4	EDX Analysis After Adsorption of Ni and MB	100
5	CONCLUSIONS AND RECOMMENDATIONS	102
5.1	Conclusions	102
5.2	Recommendations for Future Work	103
	REFERENCES	104
	APPENDICES	111

LIST OF TABLES

Table 1.1:	Acceptable Limits of Heavy Metals and Colour for Discharged Industrial Wastewater under Fifth Schedule of Environment Quality (Industrial Effluent) Regulations 2009 (Department of Environment, 2009)	18
Table 2.1:	Effective Removal Particle Size Range for Different Types of Membrane Filtration	30
Table 2.2:	Adsorption Efficiency for Different Types of Adsorbents in Optimum pH and Contact Time (Renu, Agarwal and Singh, 2017; Krishna et al., 2023; Upadhyay et al., 2021; Mashkooor, Nasar, and Inamuddin, 2020).	34
Table 2.3:	Potential Functional Groups Present in PES microcapsule	42
Table 2.4:	Comparison of Different Ranges of Process Parameters Studied for Different Types of Adsorbents.	46
Table 3.1:	Specification of Materials and Chemicals Involved	50
Table 3.2:	Specification of Instruments and Equipment Involved	51
Table 3.3:	Independent Variables and Their Ranges and Coded Levels for Ni Removal	56
Table 3.4:	Experimental Design of CCD Based on Coded Levels for Ni Removal	57
Table 3.5:	Independent Variables and Their Ranges and Coded Levels for MB Removal	58
Table 3.6:	Experimental Design of CCD Based on Coded Levels for MB Removal	59
Table 4.1:	Surface Area Analysis Results of PES Microcapsule	67
Table 4.2:	Ni Removal Efficiency Based on CCD Experimental Design Matrix	72
Table 4.3:	ANOVA Table for Ni Removal Efficiency	75
Table 4.4:	Results for Fit Statistics Table	77
Table 4.5:	Constraints Used to Optimize Ni Removal Efficiency	85
Table 4.6:	Experimental and Predicted Removal Efficiency of Ni After Optimization	86

Table 4.7:	MB Removal Efficiency Based on CCD Experimental Design Matrix	88
Table 4.8:	ANOVA Table for MB Removal Efficiency	91
Table 4.9:	Results for Fit Statistics Table	92
Table 4.10:	Constraints Used to Optimize MB Removal Efficiency	98
Table 4.11:	Experimental and Predicted Removal Efficiency of MB After Optimization	99

LIST OF FIGURES

Figure 2.1:	Chemical Structure of PES (Wasif et al., 2023)	36
Figure 2.2:	EDX Spectrum of PES membrane (Khan et al., 2021)	39
Figure 2.3:	SEM Images of PES Microspheres Using NMP Solvent by Phase Inversion (a) Surface Magnification of 100 Times (b) Surface Magnification of 10,000 Times (Lakshmi et al., 2012).	40
Figure 2.4:	SEM Cross-Sectional Images of PES Microspheres using NMP Solvent by Phase Inversion Using Magnification of 260 Times (Lakshmi et al., 2012).	40
Figure 2.5:	SEM Outer Surface Images of PES Microsphere (a) and (b) at Different Magnification Levels (Tan et al., 2023).	41
Figure 3.1:	Methodology Flow Chart	52
Figure 4.1:	SEM Images of PES Microcapsule at 40× Magnification	61
Figure 4.2:	SEM Outer Surface Images of PES Microsphere at (a) 200× Magnification (b) 370× Magnification (c) 1,000× Magnification	62
Figure 4.3:	SEM Cross Sections Images of PES Microcapsule at (a) 60× Magnification and (b) 120× Magnification	63
Figure 4.4:	SEM Cross Sections Images of PES Microsphere at (a) 300× Magnification (b) 500× Magnification (c) 1,000× Magnification	64
Figure 4.5:	EDX Results of PES Microcapsules Before Adsorption	65
Figure 4.6:	FTIR Spectra of PES Microcapsule	66
Figure 4.7:	TGA Curve of PES Microcapsule	68
Figure 4.8:	Point of Zero Charge Results of PES Microcapsule	70
Figure 4.9:	Predicted and Actual Values for Ni Removal Efficiency Response	78
Figure 4.10:	Graph of Individual Effect of pH on Ni Removal Efficiency	79
Figure 4.11:	Graph of Individual Effect of Initial Concentration of Ni on Ni Removal Efficiency	80

Figure 4.12:	Interaction Effect between pH and Initial Ni Concentration on Removal Efficiency shown as (a) a Three-dimensional Surface Plot (b) a Contour Plot	81
Figure 4.13:	Interaction Effect between Microcapsule Loading and Initial Ni Concentration on Removal Efficiency shown as (a) a Three-dimensional Surface Plot (b) a Contour Plot	83
Figure 4.14:	Interaction Effect between pH and Microcapsule Loading on Removal Efficiency shown as (a) a Three-dimensional Surface Plot (b) a Contour Plot	84
Figure 4.15:	Predicted and Actual Values for MB Removal Efficiency Response	93
Figure 4.16:	Graph of Individual Effect of pH on MB Removal Efficiency	94
Figure 4.17:	Graph of Individual Effect of Microcapsule Loading on MB Removal Efficiency	95
Figure 4.18:	Graph of Individual Effect of Initial MB Concentration on MB Removal Efficiency	96
Figure 4.19:	Interaction Effect between pH and Microcapsule Loading on MB Removal Efficiency shown as (a) a Three-dimensional Surface Plot (b) a Contour Plot	97
Figure 4.20:	EDX Results of PES Microcapsules After Ni Adsorption	100
Figure 4.21:	EDX Results of Microcapsules After MB Adsorption	101

LIST OF SYMBOLS / ABBREVIATIONS

C_f	Final concentration of wastewater sample, mg/L
C_i	Initial concentration of wastewater sample, mg/L
C_0	Center point runs
k	number of factors
AAS	Atomic Absorption Spectroscopy
ADMI	American Dye Manufacturers Institute
Ag	Argentum
As	Arsenic
BBD	Box-Behnken design
BET	Brunauer-Emmett-Teller
C	Carbon
CCD	Central Composite Design
Cd	Cadmium
Cl	Chlorine
CNTs	Carbon nanotubes
Cr	Chromium
Cu	Copper
DD	Doehlert design
DOE	Design of experiments
EDX	Energy Dispersive X-ray
EIPS	Evaporation induced phase separation
FAO	Food and Agriculture Organization
FFD	Full Factorial Design
FTIR	Fourier-transform infrared
GAC	Granular activated carbon
H	Hydrogen
HCl	Hydrochloric Acid
Hg	Mercury
IR	Infrared
MB	Methylene Blue
MWCNTs	Multi-walled carbon nanotubes

N	Nitrogen
NaCl	Sodium Chloride
NaOH	Sodium Hydroxide
Ni	Nickel
NIPS	Non-solvent induced phase separation
NMP	<i>N</i> -methyl-2-pyrrolidone
O	Oxygen
PAC	Powdered activated carbon
PAM	polyacrylamide
Pb	Lead
PE	Polyethylene
PEG	Polyethylene glycol
PEI	Polyethyleneimine
PES	Polyethersulfone
pH _{PZC}	pH value at point of zero charge
PP	Polypropylene
PSF	Polysulfone
PVDF	Polyvinylidene fluoride
PZC	Point of zero charge
RSM	Response Surface Methodology
S	Sulphur
SDGs	Sustainable Development Goals
SEM	Scanning electron microscopy
SWCNTs	Single-walled carbon nanotubes
TGA	Thermogravimetric analysis
TIPS	Thermal induced phase separation
UV-Vis	Ultraviolet-visible
VIPS	Vapour induced phase separation
WHO	World Health Organization
Zn	Zinc

LIST OF APPENDICES

Appendix A: Standard Calibration Curve of Methylene Blue	111
--	-----

CHAPTER 1

INTRODUCTION

1.1 General Introduction

Water is a basic need and a significant resource for life on Earth. The rapid growth of the global population and industrialization has led to a decrease in the availability of clean water sources and an increase in water pollution (Obaideen et al., 2022). Water is a solvent that can dissolve various organic and inorganic substances including environmental pollutants. According to Cossio et al. (2020), it was estimated that more than 95 % of wastewater in many countries was discharged into the environment without proper treatment technologies. The implementation of Sustainable Development Goals (SDGs) aims to attain a more inclusive and sustainable future for all. SDG Goal 6, clean water and sanitation, focussed on enhancing the water quality, promoting effective wastewater treatment, and ensuring the safe reuse of water resources. It stated that the water quality needs to be enhanced by decreasing pollution, eradicating the practice of waste dumping, and minimizing the discharge of hazardous chemicals and materials by the year 2030. Also, the untreated wastewater needed to be reduced and the recycling and safe reuse of water needed to be increased as well. Thus, clean and sustainable water sources can be supplied for human consumption and industrial uses after undergoing various wastewater treatments to remove heavy metals, dyes, pathogens, and other contaminants from water (Hering, 2017). Among the various organic and inorganic contaminants encountered in wastewater, heavy metals and organic dyes are the major pollutants that can pollute the aquatic environment.

Dyes are the complex organic compounds present in wastewater. For instance, industries such as textile, leather, rubber, cosmetic and printing industries can generate large amounts of coloured dye wastewater to colour their products. Due to the high demand for these industries, it is estimated that 1.6 million tonnes of dyes are produced annually and approximately 10 to 15 % of these amounts are discharged as wastewater. Improper treatment of dyes can cause health issues to the environment and living organisms and excessive exposure to dye can lead to skin irritation and respiratory problems. Some

concentrated types of organic dyes can even increase the risk of cancer in humans (Varghese, Paul and Latha, 2019).

Heavy metals are the non-biodegradable and most persistent contaminants present in wastewater. In industrial wastewater, the common hazardous heavy metals include copper, nickel, argenticum, zinc, chromium, cadmium, mercury, lead, and arsenic. Most of them will exhibit lethality and toxicity even at low trace concentrations (Akpor et al., 2014). For instance, the long-term consumption of drinking water with low levels of arsenic will increase the risk of diabetes and cancers of the lungs, liver, and bladder. In the United States Minnesota state, arsenic can be detected in water sources, and approximately 10 percent of water sources are found to have a concentration of arsenic greater than 0.01 mg/L (US Department of Health, 2022).

According to Malaysia Environmental Quality (Industrial Effluent) Regulations 2009 Paragraph 11 (1), industrial effluents must be treated and ensured that the parameters are below the limits before discharging into the water. Table 1.1 below tabulated the acceptable limits of industrial effluent, including dye or colour and heavy metals for discharged industrial wastewater. There are two standards used to specify the catchment areas of any inland waters, Standard A and Standard B. The catchment areas for Standard A are the water sources that supply for human consumption, such as drinking water, such as Sungai Muar and Sungai Johor in Johor state. The areas for Standard B are other areas that are not included in Standard A or Malaysian water. If any person or company is found to discharge industrial effluent not following the acceptable limits, the penalty or fine will be given, which is not exceeding one hundred thousand Ringgit Malaysia fine or imprisonment not exceeding five years or both (Department of Environment, 2009). For the measurement unit of colour or dye in the wastewater, the unit that will be used is ADMI, which is the American Dye Manufacturers Institute scale. It is a measurement and indicator of water quality for colour or dye in wastewater effluent to determine the contamination of dye and pigment in water (Hunter Lab, 2022).

Table 1.1: Acceptable Limits of Heavy Metals and Colour for Discharged Industrial Wastewater under Fifth Schedule of Environment Quality (Industrial Effluent) Regulations 2009 (Department of Environment, 2009)

Parameter	Unit	Standard	
		A	B
Mercury	mg/L	0.005	0.05
Cadmium	mg/L	0.01	0.02
Chromium (Hexavalent)	mg/L	0.05	0.05
Chromium (Trivalent)	mg/L	0.20	1.0
Lead	mg/L	0.10	0.5
Copper	mg/L	0.20	1.0
Nickel	mg/L	0.20	1.0
Zinc	mg/L	2.0	2.0
Silver	mg/L	0.1	1.0
Colour	ADMI	100	200

To ensure the sustainability of water, recent researchers are studying economic and environmental-friendly wastewater treatments for heavy metal ions and dye removal. For example, electrocoagulation, ion exchange, phytoremediation, and photocatalytic are the existing technologies to expel heavy metals and dyes from wastewater. Chemical-based treatments are widely used in various industries such as sugar production, pulp and paper, pharmaceutical, mining and textile industries (Sahu and Chaudhari, 2013). These industries apply coagulation treatment to treat their industrial wastewater using ferric chloride, alum, polyaluminium chloride, and chitosan as their coagulants. However, the disadvantages of using a coagulation process are increasing total dissolved salt content in treated water, inorganic coagulants, and the generation of hazardous waste. Another rising wastewater remediation used in industries is adsorption. Adsorption is a process wherein a gas or liquid molecule adheres to either a solid or liquid surface (adsorbent) and produces a thin molecular layer (adsorbate) (Lakherwal, 2014). So, the wastewater will be treated when heavy metal ions and dyes accumulate on the surface of porous adsorbents, which have a high specific surface area. It is a treatment that has low

operating cost, high removal efficiency and capacity, simplicity, a simple regeneration process, and strong applicability (Qasem, Mohammed, and Lawal, 2021).

There are different types of adsorbents that are applied in wastewater remediation to remove heavy metals and organic dyes from wastewater. They are categorised into natural, synthetic, agriculture and biopolymers adsorbents (Gupta et al., 2021). The characteristics of adsorbents can greatly affect removal efficiency, such as polarity, cost-effectiveness, surface area, and pore size distribution. The commercial adsorbents used are graphene, activated carbon, and carbon nanotubes because of their strong adsorption properties. Another potential adsorbent is polymeric microspheres, specifically PES microcapsules. Microcapsule is produced through the microencapsulation method by encapsulating adsorbing agents into the polymer for larger specific interfacial areas, higher metal selectivity, and high stability (Chen et al., 2005). PES microcapsule is a type of polymer microsphere applying the microencapsulation method, and it can contain more functional groups and active sites in the adsorption process (Lee and Patel, 2022). One of the advantages of using a polymer microsphere is enhanced material stability, mechanical properties, and adsorption capacity. PES is a special engineering polymeric material that has hydrophobic properties and can be prepared through phase inversion (da Silva Barbosa Ferreira et al., 2019). By applying PES microcapsule to remove heavy metal ions, it is expected to have good heat and chemical resistance and high adsorption efficiency.

1.2 Importance of the Study

Wastewater pollution is one of the significant environmental safety concerns worldwide because of the increase in industrial activities and urbanization. The contaminated wastewater that consists of heavy metals and dyes should not be discharged into rivers or seas intentionally.

In recent wastewater treatment, chemical-based treatments are widely used to eliminate heavy metals and organic dyes because of their low costs and ease of application. However, these separation methods require further treatment for large volumes of sludge, so they are not sustainable and environmental-friendly methods in wastewater treatment compared to

membrane filtration and photocatalytic. Furthermore, the application of membranes has fouling issues and low membrane flux (Qasem, Mohammed, and Lawal, 2021). PES membrane is a hydrophobic membrane, and this property will lead to low membrane flux and low antifouling of the membrane. Therefore, adsorption using reusable adsorbents such as PES microcapsule can be applied to adsorb heavy metal and dye ions from wastewater and prevent fouling problems (da Silva Barbosa Ferreira et al., 2019). Additionally, it has been proven that the hydrophobic and porosity of PES microcapsule can act as non-selective binding forces in adsorption (Yang et al., 2014).

1.3 Problem Statement

Many countries, including Malaysia, face various sources of heavy metals and dyes contamination, such as domestic and industry. Exposure to high-concentration heavy metals and dyes in the environment will cause bioaccumulation or pollution and possess adverse health effects on living organisms. For instance, the common hazardous heavy metals found in water sources include Cr, Ni, Zn, Pb, and Hg (Rajendran et al., 2022). Some heavy metals have high toxicity even at low concentrations and are non-biodegradable. Meanwhile, dyes produced by the textile industry can also have adverse health effects on living organisms, as they have been proven to be toxic, mutagenic, and carcinogenic (Neolaka et al., 2022). According to Zhu, Chen, and Luo (2023), organic dyes present in concentrations of less than 1 ppm can influence the solubility of gas in water and the transparency of the water. These pollutants will not be biodegraded in environment due to their complex and stable structure, and therefore will result in long-lasting threats to the environment and human health. Therefore, effective elimination of heavy metals from water sources is necessary to ensure that discharged wastewater complies with the limits regulated by the Department of Environment.

The existing heavy metals and organic dyes removal techniques used by various industries to treat the discharge of wastewater are chemical precipitation, membrane filtration, chemical oxidation or reduction, and reverse osmosis (Renu, Agarwal and Singh, 2017). These conventional techniques have limited applications and will generate a large amount of waste effluent. Also, some techniques, such as reverse osmosis and membrane filtration, are costly,

sensitive, and require specific operating conditions or maintenance. According to Renu, Agarwal and Singh (2017), adsorption is considered as the most efficient and potential technology to remove the contaminants such as dyes owing to its flexibility to be designed, reversibility, reusability of adsorbents, and high efficiency. However, there is a space for improvement that needs to further explore and investigate the efficiency of adsorption as a viable method for heavy metal removal.

The efficiency of adsorption is related to the base polymer synthesis of the microcapsules. Polymer-based microcapsules possess excellent properties in the adsorption process. Various base polymers have been studied by researchers, including polysulfone (PSF), polyamide, and polyvinylidene fluoride (PVDF) (da Silva Barbosa Ferreira et al., 2019). The properties of the polymers can greatly affect their application and lifetime. These polymers have low mechanical properties, are less resistant to heat and thermal aging, and are hard to manufacture. Thus, a possible polymer suggested to improve the properties of the adsorbents is PES.

1.4 Aim and Objectives

The purpose of this study is to develop a novel heavy metal and organic dye removal technique using PES microcapsule produced through phase inversion by adsorption. To achieve the aim of this study, the objectives are:

- i. To synthesis and characterize the polyethersulfone (PES) microcapsule via phase inversion method.
- ii. To investigate and optimize the effects of process parameters including initial concentration of heavy metal wastewater, pH, and microcapsule loading in the removal of heavy metal by PES microcapsule using response surface methodology.
- iii. To investigate and optimize the effects of process parameters including initial concentration of methylene blue (MB), pH, and microcapsule loading in the removal of MB dye by PES microcapsule using response surface methodology.

1.5 Scope and Limitation of the Study

Industrial wastewater consists of different heavy metal and organic dye pollutants and should be removed before discharging into the environment, complying with the wastewater discharged standards regulated by the government. The heavy metal that is focused on is the common metal ion present in industrial wastewater in the electroplating industry, based on various research papers. According to the company, their wastewater consists of a high concentration of nickel, which is approximately 1000 mg/L, and other heavy metals are present in trace amounts. Therefore, the heavy metal chosen for the study was nickel (Ni). Meanwhile, the organic dye chosen for the study was methylene blue (MB), which is a cationic dye.

The first step in this study involved the synthesis of the PES microcapsule through the phase inversion method. The PES polymer was chosen as the potential base polymer in this study to remove nickel and MB from wastewater using adsorption. After the PES microcapsules were prepared, the effects of various process parameters that can affect the effectiveness in removing the heavy metal were investigated according to the experimental data obtained, such as removal efficiency. The process parameters studied were initial concentration of wastewater, pH, and microcapsule loading. Moreover, the different ranges of process parameters were optimized using response surface methodology. The software that will be used for the design of experiment is Design Expert 13. As per the design, the experiments were conducted to investigate the optimized process parameter values to obtain the effective removal of heavy metals using PES microcapsule.

Furthermore, the characteristics and physical properties of PES microcapsules were examined using various instruments. The instruments are limited to scanning electron microscopy with energy dispersive X-ray spectroscopy (SEM-EDX), Fourier-transform Infrared (FTIR) spectroscopy, Brunauer-Emmett-Teller (BET) analysis, and thermogravimetric analysis (TGA) for characterization of PES microcapsules. Also, UV-Vis spectrophotometer at a wavelength of 664 nm and Atomic Absorption Spectroscopy (AAS) were used to measure the concentration of nickel wastewater and dye solution and study the adsorption efficiency in the removal of nickel and dye using PES microcapsule.

CHAPTER 2

LITERATURE REVIEW

2.1 Heavy Metal

Heavy metals can refer to metals and metalloids that are associated with environmental contamination, toxicity and harmful impacts on living things (Ali, Khan and Ilahi, 2019). It is defined as a metallic element with a density higher than 5 g/cm^3 or specific gravity higher than 5, and its atomic number should be higher than 20. Ni is a heavy metal that has a density of 8.90 g/cm^3 and atomic number of 28. According to Zaynab et al. (2022), heavy metals can be categorized into three groups based on the toxicity. The first group is the toxic heavy metals, although present in minimum concentrations. Ni is categorized under this group of metals, and it exists mostly as Ni (II) in aqueous solution, posing a threat to living organisms due to its toxicity. This group of metals is difficult to degrade through biological and photochemical processes. The second category includes heavy metals with lesser toxicity, such as bismuth and antimony. The third group comprises essential metals required in chemical or biochemical processes, such as copper and zinc.

2.1.1 Sources and Emissions of Heavy Metal

Heavy metals can be present in the environment in two ways, which are natural and anthropogenic. The increasing anthropogenic activities such as industrial, agricultural, and domestic activities can cause heavy metals to be released into the environment. According to De Beni et al. (2022), a recent estimation reported that there are approximately two million tons of industrial and agricultural waste are discharged into the water every day. Several industries generate wastewater with the presence of heavy metals, including electroplating, mining, metal smelting, petrochemicals, and paper industry (Qasem, Mohammed, and Lawal, 2021).

The electroplating industry is one of the chemical-extensive industries, and it generates high concentrations of Ni wastewater. It involves the metal coating onto the metallic plate or conducting material through the electrochemical process to prevent corrosion (Azmi et al., 2018). The elements

used in the electroplating process include Zn, Ag, Ni, Cu, Pb, and Cr. Since 1947, wastewater treatment for the electroplating industry has become a main difficulty due to its high levels of heavy metal compositions, including Ni, and effects on the environment. The wastewater has a low pH, high turbidity and high coloured (Bankole et al., 2019). The electroplating process will produce a large amount of industrial wastewater, which equals 20 % of the chemicals used in the metal and salt solution that is used in the electroplating process (Azmi et al., 2018). Thus, the wastewater consisting of a high amount of Ni heavy metals should be treated before discharging into water sources. Food and Agriculture Organization (FAO) and World Health Organization (WHO) have recommended the maximum levels and permissible limits of various heavy metals in the environment and drinking water, including Ni (De Beni et al., 2022). The recommended maximum contaminant level in irrigation water by FAO for Ni is 0.20 mg/L and the permissible limits of drinking water by WHO for Ni is 0.07 mg/L.

2.1.2 Toxicity and Health Impact of Heavy Metals

The hazard of heavy metals in water is evaluated through three characteristics, which are persistence, bioaccumulation, and toxicity (Ali, Khan and Ilahi, 2019). Toxicity can be referred to the characteristic of a substance that can influence the survival, growth, and reproduction of a living organism. When the heavy metals are discharged into the surface water, they can be converted into hydrated ions, which have higher toxicity than metal atoms (Carolin et al., 2017). The toxicity of an essential or non-essential heavy metal depends on the dosage and exposure time (Ali, Khan and Ilahi, 2019). High doses and long exposure time to some heavy metals will cause serious health impacts on humans, especially children. When the heavy metal concentration exceeds the permissible limit, the metabolism in the cell will be disrupted (Carolin et al., 2017). For Ni, it can cause lung cancer, hair loss, liver damage, liver diseases, anaphylaxis, and destroy red blood cell system.

2.2 Dyes

Dyes are aromatic organic compounds with coloration properties, capable of absorbing light and impart color to the visible spectrum. They are applied to the materials to colour them permanently, which can resist fading when exposing to water, light, oxidizing agents, and microorganisms (Khan et al., 2022). Dyes can be classified into three groups depending on their chemical structure and solubility in water. The first group is cationic dyes, such as methylene blue, malachite green, and crystal violet. The second group are anionic dyes, such as congo red, methyl orange, and alizarin yellow. The third group will be non-ionic dyes, such as dispersion orange 37 (Neolaka et al., 2022).

2.2.1 Sources and Emissions of Dyes

Dyes also can be present in the environment in two ways, which are natural and synthetic sources. The synthetic dyes will be focussed and they are more hazardous and toxic to environment and human. According to Khan et al. (2022), there are more than 100,000 commercial dyes can be found in the world and approximately 700,000 to 1,000,000 tons of dyes are manufactured every year on a global scale. Numerous dyes are applied in different industries such as textiles, food, rubber, printing, plastic, concrete, and the paper industries for many purposes. These industries will generate a large amount of coloured wastewater that consists of carcinogenic and toxic dyes that can pollute the water bodies. The coloured wastewater should be treated before discharging to the environment, so that it can be further treated for human consumption.

Among these industries, the textile industry is the largest dye consumer and manufacturer of textile dyes. One of the highest consuming dyes in the textile industry is MB dye, which will be applied to colour silk, wool, cotton and paper (Khan et al., 2022). Methylene Blue ($C_{16}H_{18}ClN_3S$) is a commonly used cationic synthetic dye that can form a stable solution with water at room temperature.

2.2.2 Toxicity and Health Impact of Dyes

Dyes have been researched and reported to affect human health and environment adversely. They are compounds that are very stable and do not decompose in the water. Thus, dyes will cause toxicity, mutagenicity, and carcinogenicity in living organisms. The exposure to dyes also will cause various diseases, such as rhodamine B can lead to the death of specialized cells in cerebral system and brainstem tissue (Neolaka et al., 2022).

The major contributors that discharge a large quantity of MB dye in water sources are textile industries, and it can become a health threat to living organisms, including humans. According to Khan et al. (2022), MB dye is toxic, carcinogenic, and non-biodegradable and it can affect human health and cause destructive effects on the environment when it is above a certain concentration. For example, it can lead to respiratory distress, abdominal disorders, blindness, and digestive diseases. Besides, the oral ingestion to MB dye can lead to several health problems, including nausea, diarrhoea, vomiting, dizziness, discoloration of urine, bladder irritation, and causing the death of premature cells in tissues. Also, it will lead to irritation of mouth, throat, stomach and digestive system. The physical contact with skin can lead to skin redness and itching.

In addition, the discharge of MB into the environment will affect aquatic life due to its toxicological reasons. MB can decrease light penetration and is a toxic source in food chains for organisms in water sources. When the MB dye is discharged into the water, it will produce highly coloured subproducts even at a very low concentration. With the reducing light penetration or sunlight transmittance, MB dye in water can decrease the solubility of oxygen and further affect the photosynthetic activity of aquatic life, and decrease the biodiversity (Khan et al., 2022). Therefore, it is important to remove the MB dye from water sources to ensure environmental sustainability.

2.3 Removal Techniques

In recent decades, various industrial wastewater treatment techniques are employed commercially to remove the heavy metals and dyes from wastewater and minimize the toxicity to living organisms and the environment. At the same time, more sustainable technologies need to be applied in the industrial sector to provide clean water. Generally, heavy metals and dyes removal techniques

can be categorized into three types of treatments, which are chemical, biological and physical techniques to remove heavy metals and dye from industrial wastewater.

2.3.1 Biological Techniques

Biological techniques involve the use of microorganisms and microbial biomass to remove pollutants from industrial wastewater. The application of biotechnology in removing heavy metals and dyes has drawn attention from industries because it is a cost-effective and eco-friendly means to treat wastewater. Potential biological techniques for eliminating heavy metals and dyes from wastewater are biosorption.

Biosorption is one of the modern heavy metals and dyes removal techniques, and it is the process of removing pollutants from a solution by adsorption using biological materials, such as bacteria, fungi, yeast, and algae. Biosorption also can be defined as the metabolically passive process of biological materials having heavy metals accumulation from wastewater using metabolic mediation or a physiochemical process (Abbas et al., 2014). The functional groups present on the microbial surface or biosorbents cell membrane walls, such as carboxyl, hydroxyl, amino, and sulfonate groups, can bind the metals and dyes through electrostatic interactions, ion exchange, and complexation (Bhatia et al., 2017). For instance, some microbial biomass can produce polysaccharides, glycoprotein and lipids, that consist of negatively charged functional groups can bind with cations to the cells through electrostatic interactions. There are some advantages of using the biosorption process in wastewater treatment, including high removal efficiency, less disposal problem, and low operating costs (Abbas et al., 2014). Also, it applies sustainable and renewable biomaterials that are cheap and capable of treating large amounts of wastewater. On the other hand, there are some disadvantages to applying biosorption commercially. The biosorption process is sensitive to properties of wastewater such as pH value, temperature, ionic concentration, contact time, presence of other ions, and suspended solids (Bhatia et al., 2017).

2.3.2 Chemical Techniques

Chemical-based techniques for heavy metals and dyes removal from industrial wastewater are mature and are widely used until now, including chemical precipitation and ion exchange (Qasem, Mohammed, and Lawal, 2021).

Chemical precipitation is a common and mature process applied in industries due to its efficiency, cost-effectiveness, process control, and flexible operating temperatures (Qasem, Mohammed, and Lawal, 2021). It is a process that transforms the organic and inorganic pollutants into solid particles for them to sediment. A chemical reagent (coagulant) will precipitate them using the effect of pH, electro-oxidation potential, or co-precipitation. The coagulant will convert cations into less soluble forms of compounds, like sulphide, hydroxide, or carbonate, so that the solid sediments can be removed easily using physical methods, such as membrane filtration (Ahmad et al., 2015). The common coagulants used for heavy metal precipitation include soda ash, caustic soda, sodium hydrosulphide, and sodium sulphide (Yadav, Singh and Jadeja, 2021). Hydroxide precipitation is preferable to be utilized due to its simplicity, adjustable pH, and cheapness. Most of the heavy metals can be eliminated using this method, including Zn, Cu, Ni, Pb, and Cr (Qasem, Mohammed, and Lawal, 2021). Also, the calcium hydroxide can be used to precipitate MB dye with removal efficiency of 77 %. The generation of sludge and high chemical cost are the major challenges of this method (Ahmad et al., 2015).

Furthermore, the ion exchange technique is a reversible chemical reaction that can substitute undesirable and toxic metal ions with lesser toxic ions. The heavy metal ion in an aqueous solution will be attached to an immobile solid particle to replace the solid particle cation. The material of solid particles used for the ion exchange method can be either natural or synthetically produced, such as inorganic zeolites and organic resins (Qasem, Mohammed, and Lawal, 2021). For dyes removal, ion exchange process also can be applied to remove dyes effectively from aqueous solution using strong interactions between charged dyes and functional groups on ion exchange resins (Ahmad et al., 2015). Organic resins have higher molecular weight polyelectrolytes to replace the mobile sites with a higher amount of exchange per unit resin. These ion exchange particles are solid and insoluble in water to absorb anions or cations from the electrolyte solution, at the same time, they release ions with the same

charge into the solution for the replacement. The ion exchange method is mainly utilized in removing low concentrations of heavy metals from aqueous solution (Yadav, Singh and Jadeja, 2021).

2.3.3 Physical Techniques

Physical techniques to remove heavy metals and dyes from industrial wastewater include membrane filtration, and adsorption.

Recently, technology advancement has progressively increased the application of membrane filtration technology in removing heavy metals and dyes from industrial effluent (Carolin et al., 2017). It is a pressure-driven separation technology using porous and thin membranes to separate the particles based on their size, applied pressure, pH value, membrane permeability, and solution concentration. Generally, the membrane can be made of ceramic and polymeric materials, such as PVDF, PE and PP, which are chemical resistance materials. Microfiltration, ultrafiltration, nanofiltration, and reverse osmosis are applied in industries to separate heavy metals and dyes from large volumes of wastewater. The microfiltration technology is used for pre-treatment to eliminate suspended solids, which are micron-sized particles. Its configurations can be either dead-end or cross-flow configurations, and it usually will be combined with other techniques to achieve higher separation efficiency. The ultrafiltration technique is a low-pressure driven and energy filtration process due to its hydrophobic properties and electrostatic interactions. However, the pore sizes of the membrane can be larger than the heavy metal ions. To tackle this issue, additives and polymeric agents can be utilized to increase the size of heavy metal ions (Carolin et al., 2017). The ultrafiltration technique also has been applied in textile industries to treat dye wastewater discharge but the application is limited. The removal efficiency of dye using this technique will not be more than 90 % (Moradihamedani, 2022). The nanofiltration filtration is a process that uses size and charge exclusions to separate the heavy metals, and it has been applied in various chemical and biotechnology industries. The polymeric nanofiltration membranes will have a positive or negative charge to improve the separation efficiency through electrostatic interactions. According to Moradihamedani (2022), nanofiltration is the most practical way to remove organic compounds with low molecular weight, which is in the range of 200 to

1000 g/mol, such as reactive dyes. However, the challenges of this method are the flux reduction and membrane fouling. Reverse osmosis is a process that requires high operating pressure to remove the heavy metal ions using a semi-permeable membrane, and only water can pass through the membrane (Carolin et al., 2017). Table 2.1 shows the range of particle sizes that can be removed effectively by different types of membrane filtration.

Table 2.1: Effective Removal Particle Size Range for Different Types of Membrane Filtration

Membrane Filtration	Removal Particle Size Range (nm)	Sources
Microfiltration	100 – 1000	(Carolin et al., 2017)
Ultrafiltration	10 – 100	(Carolin et al., 2017)
Nanofiltration	0.5 – 7	(Qasem, Mohammed, and Lawal, 2021)
Reverse Osmosis	0.1 – 1.0	(Carolin et al., 2017)

2.4 Adsorption Technology

Adsorption technique is an efficient and feasible method to remove heavy metals and dyes from industrial wastewater. De Beni et al. (2022) defined adsorption as a surface phenomenon, where the concentration of a specific substance (adsorbate), such as heavy metals and dyes present on the surface of the gas or liquid or boundary of a porous solid (adsorbent). According to Azimi et al. (2017), adsorption is a process that applies the theory of mass transfer between the liquid and solid phase, which is adsorbent. There are three main steps involved, including the diffusion from bulk solution to adsorbent surface, adsorption of the heavy metal or dye on the adsorbent surface, and transfer into the adsorbent porous structure.

The adsorption process is an alternate and promising environmental-friendly technology for the treatment of hazardous heavy metals and dye molecules due to its low operating cost, low fouling problems, ease of operation, high removal efficiency, less sludge generation, and high flexibility (Ahmad et al., 2015; Carolin et al., 2017). A wide range of adsorbents are available for the process, and they mostly can be regenerated and reused by desorption process

because adsorption is a reversible process. The adsorbents can be regenerated through several methods, such as thermal regeneration, pressure swing technique, and electrochemical regeneration (Carolin et al., 2017).

2.4.1 Adsorption Mechanism

The adsorption mechanism of heavy metals onto the adsorbents can involve different interactions, including physical adsorption, electrostatic interaction, ion exchange, surface complexation and surface precipitation. These mechanisms can differ based on the target metal ions, types of adsorbents, and environmental conditions of the solution used (De Beni et al., 2022).

Physical adsorption involves the diffusion process of heavy metals and dyes into the adsorbent pores and the deposition of particles on the surface. Several physical interactions are involved in controlling the adsorption, including polarity and steric, dipole-induced-dipole, and $\pi - \pi$ interactions. The interactions of van der Waals forces, hydrophobicity, and hydrogen bonding are also involved in the adsorption. Heavy metals and dyes will be adsorbed onto the adsorbent surface through these physical forces without undergoing the formation of chemical bonds. To ensure effective adsorption, heavy metal and dye molecules and adsorbent surfaces should have comparable pore sizes (De Beni et al., 2022).

Electrostatic interaction is a secondary interaction that will occur between heavy metal or dye ions and adsorbents, especially with the occurrence of functional groups. The heavy metal and methylene blue dye ions have a positive charge and form an electrostatic attraction with negatively charged adsorbents. Sometimes, ion exchange can occur between the adsorption of heavy metals and functional groups, which consist of oxygen elements, such as carboxyl and hydroxyl groups. Surface complexation and precipitation is a process that will produce complexes and solid precipitates (De Beni et al., 2022). Surface complexation is a formation process of different complexes where the electron pair donor interacts with the electron acceptor. Electron acceptor refers to the heavy metal ions, and the donor refers to the ions that will contribute electron pairs (Zhu, Chen and Luo, 2023).

Hydrogen bonding is a type of intermolecular interaction where a hydrogen atom will be bonded covalently to a more electronegative element

between the adsorbent and adsorbate. $\pi - \pi$ interactions occur through π electrons between the acceptor and donor molecules, which depend on functional groups in adsorbent and adsorbate. Strong $\pi - \pi$ interactions can contribute to high mechanical strength of adsorbent and strong adsorption (Zhu, Chen, and Luo, 2023).

2.4.2 Types of Adsorbents

Adsorbents are an important element in the adsorption process because they will determine the efficiency of adsorption. The removal efficiency will be affected by the surface area, pore size, surface functional groups, and polarity of the adsorbent chosen for the adsorption (Carolin et al., 2017). In industries, adsorption will be influenced by different parameters, such as adsorption mode, properties of adsorbent, dosage of adsorbent, and properties of wastewater (concentration, temperature, time, and pH). The selection of adsorbents will be based on the cost-effectiveness, impact on the environment, and adsorption properties of the specific heavy metal ions. An ideal adsorbent should be less toxic, biodegradable, low production cost, high surface area, high adsorption efficiency, reusability, high selectivity, and rapid removal of pollutants (Krishna et al., 2023). Various adsorbents have been developed for the adsorption process, including activated carbon, carbon nanotubes, chitosan, and polymeric adsorbents. Table 2.2 shows some examples of the adsorption efficiency for different types of adsorbents in optimum pH and contact time.

Activated carbon is a potential adsorbent to remove organic and inorganic pollutants because it has a high internal surface area, high porosity structure and high adaptability for adsorption. It can be obtained from carbonaceous materials, which have a high carbon content, such as coal, wood and biomass (Renu, Agarwal and Singh, 2017). Its surface area can achieve 600 – 2000 m²/g, and it is available in two types, which are powdered activated carbon (PAC) and granular activated carbon (GAC). Also, the presence of functional groups, such as hydroxyl groups, on its surface shows that it has a good adsorption affinity. For example, a type of green alga (*Ulva lactuca*) is a raw material of activated carbon, and it is able to remove copper, chromium, cadmium, and lead from wastewater with adsorption capacity of 83 to 84.7 mg/g at a maximum pH value of 5. On the other hand, the activated carbon derived

from rice husks can remove methylene blue dye at pH 10 with adsorption capacity of 578 mg/g (Neolaka et al., 2022).

Carbon nanotubes (CNTs) are the most considered adsorbents for removing heavy metals and dyes from industrial wastewater (Carolin et al., 2017). According to Krishna, et. al. (2023), they are produced from cylindrical graphite sheets with carbon atoms arranged in a hexagonal style. There are two types of CNTs available in industries, single-walled CNTs (SWCNTs) and multi-walled CNTs (MWCNTs). CNTs can be applied in many industries, including the electroplating industry, to remove Ni, Pb, Zn, Cu, Cr, and Cd. It also possesses a potential in the removal of anionic and cationic dyes from the water, such as methyl orange, Eosin B and methylene blue (Mashkooor, Nasar, and Inamuddin, 2020). CNTs can possess high chemical inertness, surface area, mechanical strength, and adsorption properties (Renu, Agarwal and Singh, 2017). They can be further processed and modified through chemical treatment and functionalized with nanoparticles to improve their adsorption capacity.

Chitosan is a natural polysaccharide derived from deacetylation of chitin through boiling of chitin in potassium hydroxide (Upadhyay et al., 2021). It is biodegradable, low cost and hydrophilic adsorbent with high adsorption efficiency. It consists of high functional groups, which are amine and hydroxyl groups, to act as active sites to form chelates with heavy metal and dye ions. However, chitosan has some disadvantages, including high crystallinity, low mechanical strength, and soluble in acidic solution (pH less than 4). Upadhyay et al. (2021) suggested that chitosan will be modified using several chemical methods, such as cross-linking, grafting, ion templating, and combination with other adsorbent materials to improve its adsorption efficiency.

Table 2.2: Adsorption Efficiency for Different Types of Adsorbents in Optimum pH and Contact Time (Renu, Agarwal and Singh, 2017; Krishna et al., 2023; Upadhyay et al., 2021; Mashkoo, Nasar, and Inamuddin, 2020).

Adsorbents	Types of Pollutants Removed	Optimum pH	Contact Time (min)	Adsorbent Dose (g/L)	Adsorbent Capacity (mg/g)	Removal Efficiency (%)
Activated carbon derived from <i>Ulva lactuca</i>	Cr	1	40	2.0	112.36	98
Composite of multi-walled carbon nanotubes (MWCNTs) and iron oxide	Cr	6	10–60	0.1–2.0	-	63 – 79
Composite of polyamine and carbon nanotubes	Pb	6	1–40	-	-	99
Polyaniline modified chitosan beads	Cd	6	120	4.5	145	99.6
Hematite and chitin core-shell nanocomposite	Pb					98.3
	Cu	5.5	-	0.5	-	90.2
	Cd					96.8
Zeolite from fly ash	Cd	6.6	1,440	10	57–195	95.6
Activated carbon derived from rice husks	MB	10	1.5	10	578.0	-
Composite of multi-walled carbon nanotubes (MWCNTs) and iron oxide	MB	6	60	1.0	42.3	-

2.5 Polymer Microcapsule

Various types of polymers, such as synthetic polymers and biopolymers can be processed to sphere-shaped micron size particles for various applications, including wastewater treatment. These microspheres or microcapsules have suitable sizes, shapes, surface areas and surface structures available for separation processes (Duraikkannu, Castro-Muñoz, and Figoli, 2021). Polymers can provide more active sites and functional groups to bind with pollutants in the adsorption process. Polymeric microspheres are applied as potential adsorbents due to their high stability and mechanical strength by protecting other materials to improve the adsorption capacity. In addition, they are non-toxic and low-cost adsorbents because they can be recycled and reused after desorption. Polymer microcapsules also can be modified to enhance their adsorption efficiency by incorporating nanocomposites into a polymer matrix, such as polystyrene. For example, sodium silicate is a synthetic polymer used to produce microspheres to adsorb lead ions from wastewater (Lee and Patel, 2022).

2.5.1 PES microcapsule

Microencapsulation is a technique to enclose micron-sized solid particles or liquid droplets or gases within an inert layer. The inert layer will separate and protect them from the surrounding. The products formed using this method are called microspheres, micro-particles, or microcapsules. Generally, the microcapsules will have a diameter range of 3 to 800 μm (Jyothi et al., 2010). The encapsulation of adsorbents is beneficial to an industry because it is easy to handle and can preserve the properties of the adsorbents for prolonged storage. Microcapsules can be defined as a spherical membrane that consists of void volume inside. Polymeric materials are widely used to prepare microcapsules through the phase inversion technique (Peña et al., 2012). One of the polymers is PES.

PES is an environmentally friendly polymeric material that has high mechanical strength and simple production, and it possesses excellent resistance to temperature, chemical, thermal aging and acidic and alkaline environment (da Silva Barbosa Ferreira et al., 2019). It has the molecular structure as shown in Figure 2.1.

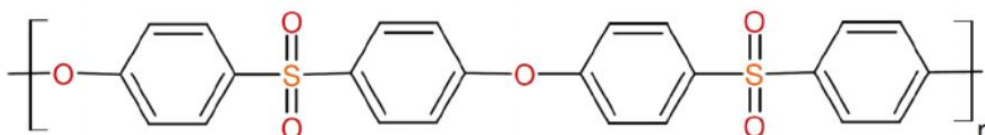


Figure 2.1: Chemical Structure of PES (Wasif et al., 2023)

From Figure 2.1, it consists of aromatic rings, which are phenyl and biphenyl groups, and they are linked by ether and sulfone groups. The role of the sulfone group is to provide high temperature resistance performance. It is widely used in industrial effluent treatment because of its enormous stacking, high surface area and active sites, specially engineered surface, water compatibility and porous structure. PES microcapsules can be reused and regenerated after the adsorption process by desorption, and it is sustainable and cost-effective adsorbents (Shi et al., 2023).

For example, the PES-based polymer can be modified with additive materials to improve its adsorption capacity and surface area as a high-performance polymeric adsorbent. Shi et al., (2023) reported that PES can be blended with PEI and iron oxides nanoparticles to remove Ni ions from wastewater. At pH 5, with microspheres loading of 50 mg and contact time of 120 minutes, the PES-PEI microspheres can achieve more than 90 % adsorption efficiency (Shi et al., 2023).

2.6 Phase Inversion Method

The phase inversion technique is the most widely used method to synthesize polymeric microcapsules. It is a demixing process which involves the transformation of homogeneous polymer solution from a liquid phase to a solid phase under controlled conditions. The transformation will be categorized into four methods based on the controlled parameter of the entire process, which are

thermal induced (TIPS), vapour induced (VIPS) and evaporation induced (EIPS), and non-solvent induced phase separation (NIPS).

The main focus of this study is NIPS because it is the most common preparation technique for polymeric membranes and microspheres. The properties of microcapsules, such as surface morphology, density, porous structure, and symmetric or asymmetric, will be affected by liquid-liquid demixing rate and diffusion rate of solvent and non-solvent. Generally, the solvent and non-solvent will diffuse across the interface and lead to the phase inversion of the polymer solution to form solid particles or precipitates (Duraikkannu, Castro-Muñoz, and Figoli, 2021). In a typical NIPS process, the polymer will be dissolved in a solvent to produce a homogeneous polymer solution. For instance, PES polymer will be dissolved in *N*-methyl-pyrrolidone (NMP) solvent to form a polymer mixture. After the polymer solution is submerged in the non-solvent coagulation bath, also known as phase inversion medium, the solvent and non-solvent are mixed spontaneously, which will decrease the free energy of the polymer. Then, the polymer will become solids or precipitates, and polymeric microspheres can be produced. The linear polymers, such as polyethylene glycol (PEG), will be added as the pore-forming agent to form the microcapsules with porous structure through NIPS. PEG is a widely used pore-forming agent because of its water solubility and polymer compatibility (Zhang et al., 2022). NIPS method requires strong organic solvents to dissolve the PES polymer solution because the PES possesses high chemical resistance. The potential solvents are NMP, dimethylacetamide, and dimethylformamide. The polymers such as PES, PSF, and PVDF require solvents with strong polarity for phase inversion. NMP is one of the commonly used solvents that has strong polarity and high solubility in polymer solution (Wang et al., 2019). Therefore, the synthesis of PES microcapsules will utilize the NMP solvent in a non-solvent coagulation bath, which is water through phase inversion using the NIPS method.

2.7 Characterization Studies of PES Microcapsule

The characterization studies of PES microcapsules are important to study the functional and morphological properties, such as particle sizes, shapes and internal structures. There are different experimental characterization techniques

for PES microcapsules will be used in this study to investigate their properties, including the pH drift method, scanning electron microscopy with energy dispersive X-ray spectroscopy (SEM-EDX), Fourier-transform infrared (FTIR) spectroscopy, Brunauer-Emmett-Teller (BET) analysis, and thermogravimetric analysis (TGA) (Mourdikoudis, Pallares, and Thanh, 2018).

2.7.1 pH drift method

The pH drift method is used to evaluate the point of zero charge (PZC or pH_{PZC}) in the characterization of the adsorbent, which is the PES microcapsules, and to evaluate the surface charge of the PES microcapsule. The PZC is defined as the pH value at which the adsorbents have a net zero surface charge, which indicates that there are equal amounts of both positive and negative charges at the surface of the adsorbent. This method is to study the interaction between the adsorbent surface and charged species in the solution because the pH of the solution will affect the surface properties of microspheres (Aktar et al., 2023). The adsorption of the cationic species is preferable when the surface of the adsorbent is negatively charged due to the solution pH, which is greater than the pH value at PZC (pH_{PZC}) (Mehdi and Aravamudan, 2022).

When the solution pH is below PZC, the surface charge of adsorbent is positive, while above the PZC will produce a negatively charged surface. The pH is expected to be higher than PZC because the surface of the PES microcapsule should be negatively charged for it to bind with cationic ions (Mehdi and Aravamudan, 2022). For instance, a silica gel modified with vanadium (V) oxide is applied as the adsorbent for the removal of Ni ions. The pH value at PZC of modified silica gel was 2.92. When the pH is above 2.92, it indicates that the adsorbent will have a negative surface charge to increase the affinity towards heavy metal ions and adsorption efficiency (Sulejmanović et al., 2022).

2.7.2 SEM-EDX

SEM-EDX is widely used to observe surface morphology, chemical composition, and structure of nano-scaled particles. It is an electron microscope that applies a concentrated beam of electrons with high energy generated from an electron gun to emit signals to the surface of the solid material. A detailed

three-dimensional and topographical image can be produced that shows the selected surface area of the solid material. The magnification of SEM can range from 20 times to 30,000 times, and some advanced SEM can achieve 1,000,000 times the original sizes. It can produce high-resolution images at higher magnification levels. However, SEM can be interfered with by electric, magnetic, and vibration signals and these can affect the image formed is distorted (Mallakpour and Rashidimoghadam, 2019). In addition, EDX analysis is a technique coupled with electron microscopy that uses generation of X-rays to detect the presence of elements in the sample. It will produce a spectrum that will show the position of a peak, and identify the elements (Scimeca et al., 2018). The area under the peak is directly proportional to the number of atoms of the element in the irradiated area. For example, the elements presence in PES microcapsule are C, S, and O and these three elements can be detected using EDX and their chemical composition will be known. Figure 2.2 shows the possible elements that will present in PES before treatment using EDX analysis, which are C, O, and S.

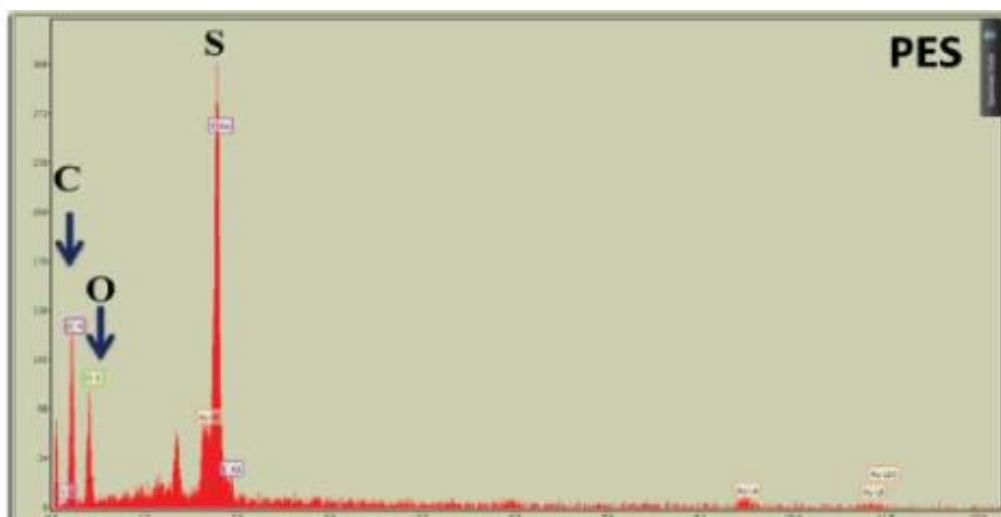


Figure 2.2: EDX Spectrum of PES membrane (Khan et al., 2021)

According to Lakshmi et al., (2012), the PES microcapsules are synthesized using NMP solvent and 10 wt% of PES polymer solution through phase inversion. The outer surface of the microsphere was observed under SEM at 20 kV and shown in Figure 2.3 below. The researchers used nitrogen liquid to freeze the microspheres and produce a clean cross-sectional view of the microsphere, as shown in Figure 2.4.

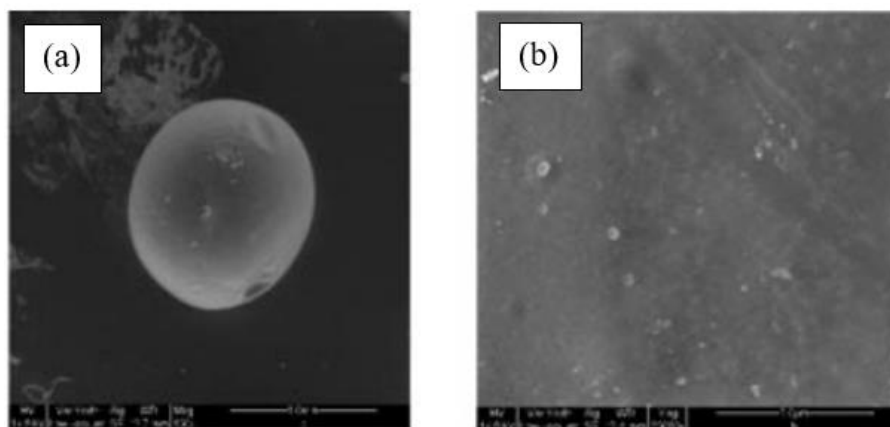


Figure 2.3: SEM Images of PES Microspheres Using NMP Solvent by Phase Inversion (a) Surface Magnification of 100 Times (b) Surface Magnification of 10,000 Times (Lakshmi et al., 2012).

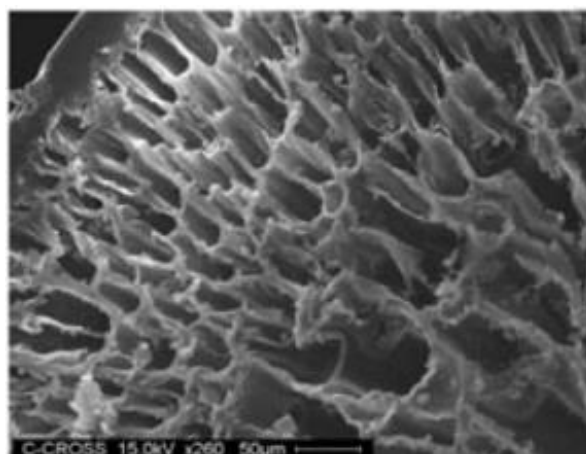


Figure 2.4: SEM Cross-Sectional Images of PES Microspheres using NMP Solvent by Phase Inversion Using Magnification of 260 Times (Lakshmi et al., 2012).

According to Tan et al., (2023), PES microspheres were produced using 10 wt% of PES polymer solution, 5 wt% of polyethylene glycol, and NMP solvent through phase inversion. In Figure 2.5, the outer surface of the microcapsule was observed using SEM at different magnification levels.

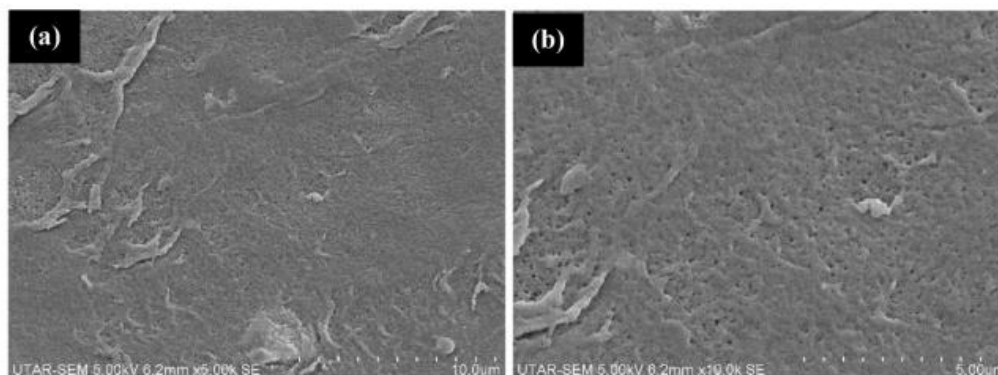


Figure 2.5: SEM Outer Surface Images of PES Microsphere (a) and (b) at Different Magnification Levels (Tan et al., 2023).

2.7.3 FTIR

FTIR is an analytical method applied to detect the functional groups, such as hydroxyl and molecular bonding present in a sample through infrared (IR) radiation (Guerrero-Pérez and Patience, 2020). The compounds with changing of dipole moments during the vibration will absorb the IR radiation to determine the functional groups based on their wavelengths. Then, the Fourier Transform signal forms a spectrogram, and it will produce the plot of absorbance against wavelength (700 – 400,000 nm) or wave numbers (14,000 – 25 cm^{-1}). There will be an absorption spectrum which shows a fingerprint or peak pattern, and the molecules can be identified from the wave numbers. Table 2.3 shows the potential functional groups that will present in a PES microcapsule. The analysis is suitable for different states of the sample, including liquid, solid, gas, and powders (Tkachenko and Niedzielski, 2022). Therefore, the synthesized PES microcapsule will be characterized using FTIR to identify the functional groups present.

Table 2.3: Potential Functional Groups Present in PES microcapsule

Functional Group	Absorption Band (cm^{-1})	Sources
Water O—H stretch	3700 – 3100	(Guerrero-Pérez
Carboxylic acid O—H stretch	3000 – 2500	and Patience,
Aromatic C=C stretch	1700 – 1500	2020)
C—O—C stretch	1250 – 1050	
Ethers C—O group	1300 – 1000	(Mohamed et
Amines C—N stretch	1350 – 1000	al., 2017)
N—H bend (primary and secondary)	1640 – 1550	(Mohamed et
S=O Sulfones group	1375 – 1140	al., 2017)

2.7.4 BET

BET is an analysis technique that can measure the specific surface area in m^2/g and pore size distribution of a substance through the physical adsorption of gas molecules on a porous solid surface (Nasrollahzadeh et al., 2019). BET theory mechanism applies to systems involving multilayer adsorption and normally uses non-reactive probing gases as adsorbates to measure the specific surface area. It applies the Langmuir theory by only assuming a layer of adsorbate (Barhoum and García-Betancourt, 2018). There are several adsorbates applied for surface probing to provide a wide range of different operating temperatures and measurement scales, including nitrogen (Nasrollahzadeh et al., 2019). Nitrogen is the adsorbate that is widely used for probing gas, and the standard BET method is commonly performed at the boiling temperature of nitrogen. The methodology of BET consists of a few operating steps. The porous sample is outgasses, and an inert gas such as nitrogen will be conditioned by adjusting the operating temperatures (Barhoum and García-Betancourt, 2018). The measurement of adsorption isotherms will be measured according to a varied specific pressure, which is within the range of 0.05 and 0.3. So, the specific surface area and porous size of a PES microcapsule will be evaluated using BET.

2.7.5 TGA

TGA is also one of the analytical techniques used to evaluate the thermal stability of a material and quantify its volatile fraction components by observing the change in weight when the sample is heated at a constant rate (Rajisha et al., 2011). Then, the measurement will be conducted in atmosphere air or inert conditions, such as helium and argon, so the plot weight percent against increasing temperature can be plotted. TGA contains a weight balance with high sensitivity to measure the weight changes and a furnace to heat the sample (Ebnesajjad, 2011). It uses a platinum heating element to heat the sample to a temperature of up to 1,000 °C. Thus, TGA is able to measure the thermal stability of a material with high temperature and high weight balance sensitivity of 0.1 µg in the controlled heating rate. The heating rate of TGA under atmospheric air and inert gas can vary from 0.1 °C – 200 °C/min. In this study, TGA will be used to measure the thermal stability of the PES microcapsule and determine its decomposition temperature.

2.8 Effects of Process Parameters

There are several factors that can influence the adsorption of heavy metals and dyes, such as adsorbent dose (loading), initial concentration, and solution pH. The highest adsorption efficiency of heavy metal and dye ions can be achieved when these parameters are optimized (Jadoun et al., 2022). In this study, the factors that will be studied are pH, PES microcapsule loading, and initial concentration.

2.8.1 Effect of pH

The first factor that can affect the elimination efficiencies of heavy metals and dyes is the solution pH value. The pH of the wastewater sample can affect ionization degree and surface properties of the adsorbent, which is PES microcapsules. The ionization of the functional groups on the adsorbent will determine adsorbent surface charge to attract or repel the cationic ions. When the solution pH is low, the active sites will be protonated, and the surface charge of the adsorbent will be positively charged. The positively charged surface and positive charged heavy metal ions will have repulsive interactions and cause low adsorption efficiency. For the dyes, the pH also plays the same role, the

surface of the adsorbent in solution will be protonated when the solution is acidic and there will be a repulsive force between cationic dye and adsorbents (Rápó and Tonk, 2021). Therefore, the higher pH of the solution is preferable for binding of cations with the negatively charged binding sites of the adsorbent to achieve higher adsorption efficiency (Jadoun et al., 2022).

For example, the removal efficiency of lead ions is 9.9 % at pH 2 using polythiophene- Al_2O_3 adsorbents. When the pH of the solution is increased to pH 6, the removal efficiency will be increased to 89.9 %. Polymer-based adsorbents, such as polyaniline and polypyrrole, were found to have the highest removal efficiency of heavy metal ions from wastewater at a pH range of 6 to 8 (Jadoun et al., 2022). It shows that the removal of heavy metal ions favours the high pH environment. On the other hand, the removal efficiency of methylene blue using polyacrylamide (PAM) microspheres can achieve up to 90 % at pH 8 with 10 mg/L of initial concentration and 5 mg of adsorbent (Yao et al., 2015).

2.8.2 Effect of Microcapsule Loading

The amount of adsorbent is important to be optimized to obtain the highest removal efficiency of heavy metals and dyes from wastewater. It will determine the equilibrium between adsorbent and adsorbate and affect the cost of dosing the adsorbent (Soliman and Moustafa, 2020). Generally, increasing of adsorbent dosage or microcapsule loading will increase adsorption efficiency due to higher surface area, and more active sites will be available for adsorption until a maximum limit and achieve constant after the limit. The adsorption efficiency will decrease when the active sites aggregate because of the decrease in the available surface area for the adsorption. Thus, the minimum microcapsule loading is needed to achieve maximum removal efficiency (Jadoun et al., 2022).

For example, the increasing of adsorbent loading from 1.0 g/L to 5.0 g/L can increase the removal efficiency of lead ions from 25.8 % to 89.7 % using activated carbon combined with iron oxide magnetic composite adsorbent (Jadoun et al., 2022). Another researchers, Soliman and Moustafa (2020), found that the increasing of expanded perlite adsorbent loading from 1.0 g/L to 8.0 g/L and 1.0 g/L to 10.0 g/L to remove Ni ions increased the adsorption efficiency from 43 % to 90.5 %. After this dosage is added, the adsorption efficiency becomes constant. The increasing trend shows that more adsorbent surface area

and active sites are available for the heavy metal ions to be adsorbed with the increased adsorbent loading. After achieving the maximum limit, the adsorption efficiency is constant because the definite amount of heavy metal ions is bound with active sites because the initial concentration of the ions in the solution is constant. The increasing adsorbent loading will not cause the increase of heavy metal ions bound with the adsorbent surface. For the dye removal, the removal efficiency of MB dye will be increased from 45.16 % to 96.00 % when the fly ash adsorbent loading is increased from 8 g/L to 20 g/L (Oladoye et al., 2022).

2.8.3 Effect of Initial Concentration

Another factor that will affect the adsorption efficiency is initial concentration of heavy metal. When the initial concentration of metal ions is increased, it will cause a decrease in adsorption efficiency. It is because the saturation of adsorption sites on the surface of adsorbent will occur. However, the adsorption capacity will be increased because of the higher driving force for mass transfer between the aqueous and bulk phase at a higher initial concentration of heavy metal ions. The efficiency depends on the possible interactions between the available active sites on the adsorbent surface and metal ions. At a low initial metal ion concentration and high adsorbent dosage condition, the final concentration of the solution will drop easily at a lower level to achieve equilibrium and the active sites will remain in unsaturation condition.

According to the research conducted by Hellal et al. (2023), the researchers used sodium alginate beads to encapsulate nanoparticles, which is zeolite sony mobile-5 as adsorbents to remove Ni (II) from the solution. The adsorption studies investigated four parameters, which are pH, initial metal ion concentration, temperature, and adsorbent dosage. The range of pH was 4 to 7, with initial metal ion concentration of 20 to 100 mg/L and 4 to 24 g/L adsorbent dosage. The Ni removal efficiency was reduced from 93 % to 86 % when the initial metal concentration was increased from 20 to 100 mg/L at room temperature of 25 °C and dosage of 8 g/L. Table 2.4 below shows the comparison between different ranges of process parameters studied by different researchers for adsorption studies and these data are useful when designing the adsorption experiment using PES microcapsule.

Table 2.4: Comparison of Different Ranges of Process Parameters Studied for Different Types of Adsorbents.

Adsorbate	Adsorbents	pH	Contact Time (min)	Adsorbent Dose (g/L)	Initial Concentration (mg/L)	References
MB	Polyacrylamide (PAM) Microspheres	2 – 10	300	0.25	5 – 300	(Yao et al., 2015)
	Polydopamine (PDA) Microspheres	2 – 10	10 – 120	0.50	30 – 100	(Fu et al., 2015)
Ni (II)	Hydrochar and Activated Carbon Microspheres from Tangerine Peels	3 – 9	15 – 1440	2.50	5 – 100	(De Tuesta et al., 2022)
Pb (II)	Polymeric Microspheres of Methacrylic Derivatives of Aromatic Thiols	2 – 5	1 – 360	5.00	25 – 500	(Fila et al., 2019)
Ni (II) and Cu (II)	Modified Mangrove Barks	2 – 10	10 – 180	2 – 60	10 – 100	(Rozaini et al., 2010)

2.9 Response Surface Methodology (RSM)

Design of experiments (DOE) is a systematic and efficient approach applied to study the relationships between multiple factors affecting an experiment and the responses or results (Karimifard and Moghaddam, 2018). When designing an experiment, DOE can be used to change all factors involved simultaneously and interpret the results using mathematical models. If DOE is not used in designing the experiment, there will be only one of the factors will be analysed, and other factors are assumed to be constant throughout the experiment. The disadvantages of this method are longer time to collect the data and large amount of experimental runs required. Also, the interactions between the process parameters will not be able to be analysed. From the sustainability point of view, the execution of minimum experiment runs can consume a lower amount of materials and less laboratory work in conducting the experiment resulting in lower experiment costs and lesser waste produced.

Among DOE approaches, RSM is widely used in designing the experiments, modelling and optimizing the experimental parameters. RSM is a compilation of statistical and mathematical techniques applied for experiment designs and model development by investigating the interactions of different parameters and process optimization (Karimifard and Moghaddam, 2018). RSM involves fitting mathematical models, such as linear, quadratic, cubic, and polynomial functions, to the experimental data obtained from a set of design of experiments. Then, the statistical models will be applied to verify the model obtained. The optimization of process parameters or experimental conditions can be determined through RSM. The process parameters and their ranges need to be chosen in a suitable range when designing the experiments to prevent unreliable and uninformative final results. Therefore, in this study, the effects of different process parameters or factors that affect the adsorption efficiency can be investigated using RSM. The adsorption efficiency in removing heavy metals using PES microcapsule is mostly influenced by several process parameters, including pH, initial concentration, and microcapsule loading.

There are some available design strategies under RSM, which are full factorial design (FFD), CCD, Box-Behnken design (BBD), and Doehlert design (DD) (Karimifard and Moghaddam, 2018). CCD is the design method that is widely used in designing the experiments and optimization. It can create a

quadratic response surface model and predict the interaction effects of process parameters. It is preferable to be used because it can generate lesser experimental runs, which reduces the waste produced during the experiment. In CCD, there are three types of points required to generate the total number of experimental runs, which are center points, axial points and factorial points. Therefore, the determination of the total number of experimental runs can be obtained from Equation 2.1.

$$\textit{Total Number of Experimental Runs} = 2^k + 2k + C_0 \quad (2.1)$$

where k is number of factors, 2^k is factorial runs, $2k$ is axial runs, and C_0 is center point runs. From Equation 2.1, it illustrates that with the increasing independent factors or process parameters in the experiment, the total experimental runs for the complete design will be increased as well.

Design Expert is a statistical software which can help to conduct a CCD to optimize the independent factors involved in the adsorption experiment so that it can give maximum adsorption efficiency (Sopyan, Gozali and Guntina, 2022). In this study, Design Expert version 13 will be applied for performing the design of experiments and generating the experimental runs with different levels using RSM.

CHAPTER 3

METHODOLOGY AND WORK PLAN

3.1 Introduction

This chapter will include all methodologies required to be conducted to achieve the objectives of this study. The methodologies include the synthesis of PES microcapsule, characterization of PES microcapsule adsorbent, adsorption experiment on removing Ni from electroplating wastewater, adsorption experiment on removing MB dye, optimization of process parameters using response surface methodology, and investigation of the effects of process parameters on adsorption experiment. The materials and equipment involved in the experiment are listed in this chapter. A methodology flowchart is presented in Figure 3.1 to show the overall process flow of the study.

3.2 Materials and Chemicals

Table 3.1 tabulated the materials and chemicals involved in this study. The wastewater sample was received from the electroplating industry.

Table 3.1: Specification of Materials and Chemicals Involved

Chemicals	Purity (%)	Brand/Source	Usage
Polyethersulfones (PES)	> 99.0	BASF, Malaysia	Synthesis of PES microcapsule
Polyethylene glycol (PEG)	> 99.5	Chemicals Solutions Sdn. Bhd., Malaysia	Pore forming agent
<i>N</i> -methyl-2-pyrrolidone (NMP)	> 99.9	Merck, Malaysia	Solvent
Deionized water	-	UTAR Lab	Coagulation bath and Dilution
Distilled water	-	UTAR Lab	Dilution
Sodium Hydroxide (NaOH)	> 99.0	Merck, Malaysia	pH adjustment
Hydrochloric Acid (HCl)	37.0	Sigma-Aldrich, Malaysia	pH adjustment
Sodium Chloride (NaCl)	> 99.5	Merck, Malaysia	pH drift method
Methylene Blue (MB)	-	R&M, Malaysia	Model Pollutant

3.3 Equipment

The instrument and equipment required in this study are tabulated in Table 3.2.

Table 3.2: Specification of Instruments and Equipment Involved

Equipment	Model	Usage
Hotplate stirrer	-	To heat and stir polymer solution
Peristaltic Pump	Masterflex L/S 77200-60	To channel the polymer solution to a syringe needle
pH meter	-	To measure pH value of wastewater sample
SEM-EDX	Hitachi, S-3400 N	To characterize surface morphology
FTIR	Nicolet iS10	To characterize functional groups
BET	Micromeritics, 3Flex	To characterize specific surface area and pore size
TGA	Thermo Scientific Sorptometric, SO1990	To characterize thermal stability of PES microspheres
UV-Vis Spectrophotometer	Varian, Cary 100	To measure dye concentration
AAS	AAAnalystTM 200, PerkinElmer Inc.	To measure Ni concentration
Orbital Shaker	-	To shake the solution during adsorption experiment
Oven	Memmert UFB500	To dry the PES microcapsule

3.4 Overall Process Flow Chart

Figure 3.1 below shows the overall process flow chart of the experiment. The experimental study started with the synthesis of PES microcapsules using phase inversion. Then, the characterization studies of the synthesized PES microcapsule were conducted. After that, the adsorption experiment was studied and the initial and final concentrations of methylene blue in water and electroplating wastewater were measured using a UV-Vis spectrophotometer at 664 nm and AAS. Next, the optimization of the experiment using RSM was conducted to study the effects of different process parameters, including pH, initial concentration and microcapsule loading, on adsorption efficiency. Finally, the adsorption efficiency of the PES microcapsules was determined.

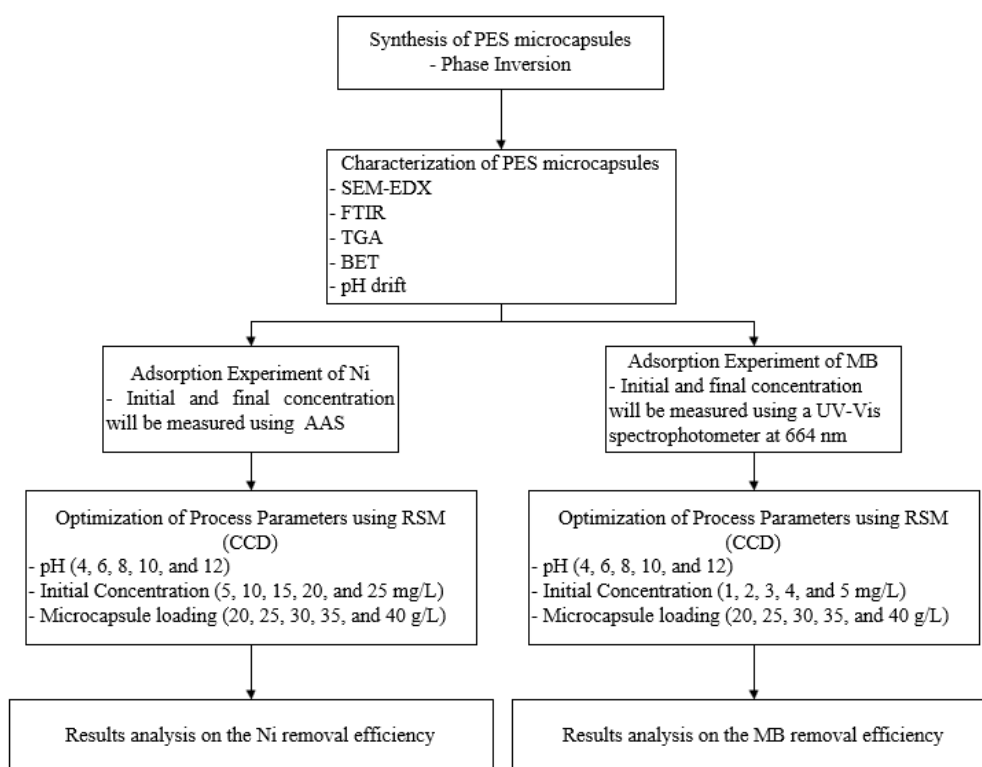


Figure 3.1: Methodology Flow Chart

3.5 Synthesis of PES Microcapsules

Firstly, the materials needed were PES, PEG and NMP solvent. The PES polymer solution was prepared by dissolving 15 wt% of PES and 5 wt% of PEG in 80 wt% of NMP solvent. The PEG functions as a pore-forming agent. 15 wt% of PES was used because it was found that it can give the highest porosity and specific surface area. 5 wt% of PEG was used because it can produce larger pore diameter of PES microcapsules. Then, the mixed solution was subjected to a constant stirring speed at 250 rpm and heated at 70 °C for two hours. After that, the solution was immediately left to cool to room temperature of 25 °C to ensure that the polymer solution was fully dissolved to produce a homogenous solution. The solution was channelled through a syringe needle with size 26 G to produce PES microcapsules at the pumping rate of 0.4 mL/min using a peristaltic pump. Therefore, a dropwise addition of PES polymer solution was performed into a coagulation bath, which was deionized water to produce microcapsules. The PES microcapsules were formed as precipitates through the phase inversion technique, and they were collected and rinsed with deionized water (Tan et al., 2023). The oven was used to dry PES microcapsules with a temperature of 55 °C for two hours. Phase inversion occurred when the PES polymer solution was submerged in a coagulation bath consisting of non-solvent (deionized water). Thus, the region between solvent and non-solvent was exchanged and precipitates, where PES microcapsules were formed (Yee et al., 2021).

3.6 Characterization of PES microcapsules

Characterization studies, including SEM-EDX, BET, FTIR, TGA, and pH drift were carried out on the PES microcapsules adsorbents.

3.6.1 SEM-EDX

SEM-EDX equipment with the brand of Hitachi, S-3400N was used to observe the surface morphological structure of the microcapsules at 15.0 kV accelerating voltage. The sample preparation was conducted by placing the PES microspheres on the specimen holder with carbon tape. The samples were subjected to a sputter coater to coat them with gold and palladium, and they were placed into the SEM-EDX equipment. The desired magnified image of the samples was captured. For the EDX analysis, the elements of carbon (C),

oxygen (O), and sulphur (S) were chosen to be observed. The graph of EDX analysis was obtained.

3.6.2 BET

BET analysis using surface analyzer (Micromeritics, 3Flex) was used to determine the pore sizes and specific surface area of the PES microcapsules. The sample preparation was carried out by placing PES microcapsules into a sample tube. The degassing process started at 90 °C for an hour and the sample analysis was run at 100 °C for 8 hours with a temperature ramp rate of 10 °C/min.

3.6.3 FTIR

FTIR spectrophotometer (Nicolet iS10) was used to determine the functional groups present in PES microcapsules at a range of 4000 to 400 cm^{-1} . The sample was placed on the sample holder and scanned using infrared light. The peaks generated were compared with literature to identify the specific functional groups.

3.6.4 TGA

Besides, TGA with the brand of Thermo Scientific Sorptometric, SO1990 was used to determine the thermal stability and decomposition temperature of the PES microcapsules at a temperature range of 30°C to 1000 °C with a temperature ramp rate of 10 °C/min under nitrogen gas. The PES microcapsule was placed in the sample pan and the analysis was run for two hours.

3.6.5 pH drift

To determine the surface charge of the microcapsules, the pH drift method was used by adding 50 mg of PES microcapsules into different pH values of prepared 0.1 M NaCl solution. The 0.1 M sodium hydroxide and 0.1 M hydrochloric acid was used to adjust the pH to 2, 4, 6, 8, and 10. The solutions were mixed well for 48 hours to ensure equilibrium. The initial and final pH of each solution was recorded, and the graph of the final pH against the initial pH was plotted (Tan et al., 2023).

3.6 Preparation of Ni Stock Solution and MB Stock Solution

The preparation of Ni stock solution from industrial wastewater was conducted. Firstly, the initial concentration of the Ni wastewater from the electroplating industry was measured, and the initial concentration was 1292 mg/L. Then, the stock solution was prepared by diluting the wastewater to 100 mg/L using deionized water in a 100 mL volumetric flask. For the adsorption experiment, 5 mg/L, 10 mg/L, 15 mg/L, 20 mg/L, and 25 mg/L were studied. Thus, the stock solution was diluted to different concentrations as the initial concentration of Ni wastewater. Each initial concentration of Ni solution was measured using AAS to have an accurate value of the initial concentration of Ni solution. On the other hand, the preparation of MB stock solution was conducted by diluting 800 mg/L of MB dye to 10 mg/L with distilled water. The calibration curve was prepared by diluting the 10 mg/L of stock solution into 0.2 mg/L, 0.4 mg/L, 0.6 mg/L, 0.8 mg/L, 1.0 mg/L, and 2.0 mg/L. A UV-Vis spectrophotometer was used to measure the initial dye concentration at a wavelength of 664 nm.

3.7 Design of Experiment Using Response Surface Methodology

CCD was used to study the interaction between three process parameters that can affect the Ni and MB removal efficiency using PES microcapsules adsorbent. The three independent variables are pH (X_1), microcapsule loading (X_2), and initial concentration (X_3). The response variable was the removal efficiency of heavy metal Ni and MB dye.

Firstly, the desired ranges of each variable studied for Ni removal was determined. The effect of solution pH on the removal efficiency of Ni was studied by varying the pH value of the wastewater sample. The pH of the wastewater was manipulated in the range of 4 to 12. The pH adjustment to the desired value was conducted using 0.1 M HCl and 0.1 M NaOH solution. Moreover, the effect of microcapsule loading was investigated by varying the weight of the PES microcapsule based on the volume of the wastewater sample in unit of g/L from 20 g/L to 40 g/L. The studied range of initial concentration of Ni solution was 5 mg/L to 25 mg/L. Besides, the contact time was not studied in the experiment and it was set to 5 hours, which was an average time for adsorption of Ni.

For MB dye adsorption study, the desired ranges of each variable studied was similar to Ni adsorption. The pH of the dye was manipulated in the range of 4 to 12. The pH adjustment was done using 0.1 M HCl and 0.1 M NaOH solution. The effect of microcapsule loading was investigated by varying the weight of the PES microcapsule based on the volume of the dye solution from 20 g/L to 40 g/L. The studied range of initial concentration of MB solution was 1 mg/L to 5 mg/L. Besides, the contact time was set to 5 hours, which was same with the Ni adsorption to make sure the adsorption of MB dye can achieve equilibrium.

There are five levels were used to generate the total number of experimental runs in CCD, which were -2, -1, 0, 1, and 2. The coded levels of the independent variables were set according to the studied ranges. Based on the CCD model, the total number of experimental runs were 20 runs for Ni adsorption study and another 20 runs for MB dye adsorption study.

Table 3.3 shows the independent factors (pH, microcapsule loading, and initial concentration) and their coded levels for Ni removal.

Table 3.3: Independent Variables and Their Ranges and Coded Levels for Ni Removal

Parameters	Variable	Ranges and Coded Levels				
		-2	-1	0	1	+2
pH	X_1	4	6	8	10	12
Microcapsule loading (g/L)	X_2	20	25	30	35	40
Initial Ni Concentration (mg/L)	X_3	5	10	15	20	25

According to the experimental runs generated, the adsorption experiments were conducted to study the Ni removal efficiency. Table 3.4 tabulated the experimental runs generated using CCD.

Table 3.4: Experimental Design of CCD Based on Coded Levels for Ni Removal

Run	X_1: pH	X_2: Microcapsule loading (g/L)	X_3: Initial Ni Concentration (mg/L)
1	8	20	15
2	8	30	15
3	8	30	15
4	10	35	20
5	8	30	25
6	8	30	15
7	10	25	20
8	6	25	20
9	10	35	10
10	8	30	5
11	12	30	15
12	10	25	10
13	4	30	15
14	6	25	10
15	8	30	15
16	8	30	15
17	6	35	20
18	8	30	15
19	8	40	15
20	6	35	10

Table 3.5 shows the independent factors (pH, microcapsule loading, and initial MB concentration) and their coded levels for MB removal.

Table 3.5: Independent Variables and Their Ranges and Coded Levels for MB Removal

Parameters	Variable	Ranges and Coded Levels				
		-2	-1	0	1	+2
pH	X_1	4	6	8	10	12
Microcapsule loading (g/L)	X_2	20	25	30	35	40
Initial MB Concentration (mg/L)	X_3	1	2	3	4	5

According to the experimental runs generated, the adsorption experiments were conducted to study the MB removal efficiency. Table 3.6 tabulated the experimental runs generated using CCD.

Table 3.6: Experimental Design of CCD Based on Coded Levels for MB Removal

Run	X_1: pH	X_2: Microcapsule loading (g/L)	X_3: Initial MB Concentration (mg/L)
1	6	25	4
2	8	40	3
3	10	35	4
4	8	30	5
5	10	35	2
6	4	30	3
7	6	35	4
8	8	30	3
9	8	20	3
10	10	25	4
11	6	25	2
12	6	35	2
13	8	30	3
14	8	30	3
15	8	30	3
16	8	30	3
17	10	25	2
18	8	30	3
19	8	30	1
20	12	30	3

After obtaining the experimental runs, the adsorption experiments were started. The initial and final concentration of the Ni wastewater sample was measured using AAS. Meanwhile, the initial and final concentration of MB dye was measured using a UV-Vis spectrophotometer at a wavelength of 664

nm. The synthesized PES microcapsules were added into 30 mL of different concentrations of Ni wastewater sample (5 to 25 mg/L) and MB dye solution (1 to 5 mg/L) with different pH of the solution (4 to 12) and different microcapsule loading (20 to 40 g/L) for a contact time of 5 hours. During the adsorption, the different sets of runs were placed on the orbital shaker to mix the PES microspheres well in the Ni and MB solution.

3.8 Results Analysis

The Ni and MB removal efficiency from the wastewater and dye sample was calculated based on Equation 3.1. The initial concentration and final concentration of the wastewater and dye were measured using the AAS for Ni and UV-Vis Spectrophotometer at a wavelength of 664 nm for methylene blue for each experimental run.

$$\text{Removal Efficiency (\%)} = \frac{C_i - C_f}{C_i} \times 100 \% \quad (3.1)$$

Where

C_i = Initial Concentration of Ni or MB Sample (mg/L)

C_f = Final Concentration of Ni or MB Sample (mg/L)

CHAPTER 4

RESULTS AND DISCUSSION

4.1 Characterization Studies of PES Microcapsule

After synthesizing the PES microcapsules using the phase inversion method, several characterization techniques were studied to investigate the properties of PES microcapsules, including SEM-EDX, surface area analysis, FTIR, TGA, and pH drift method. The characterization studies are to study the surface morphology, functional groups present, surface area, pore size, thermal stability, and surface charge of the PES microcapsules.

4.1.1 SEM-EDX

The surface morphologies of PES microspheres were examined and observed using SEM equipment.

Figure 4.1 shows PES microcapsules were observed at a magnification of 40 \times . It can be observed that the PES microcapsule produced was spherical in shape. Its outer surface was rather smooth, and it consisted of a few tiny pores on the surface.

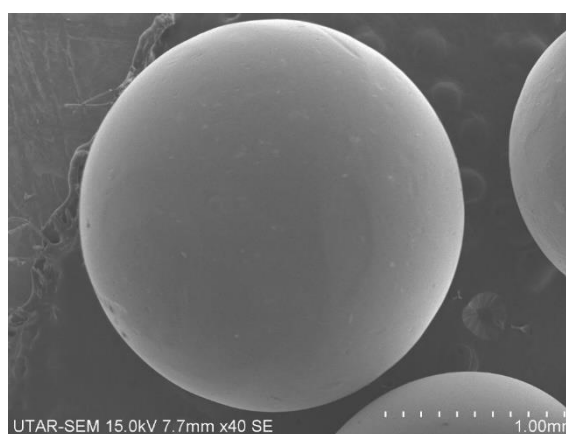


Figure 4.1: SEM Images of PES Microcapsule at 40 \times Magnification

According to research conducted by Tan et al. (2023), the PES polymer concentration could affect the structure formed of PES microcapsules and the range of concentration that can form spherical shape microcapsules is between 10 wt% and 15 wt%. The higher the PES polymer concentration, the higher the

viscosity of the polymer solution. Also, the selection of 5 wt% pore-forming agent, PEG concentration, was due to it providing a larger pore diameter and specific surface area. In this study, it was proven that the spherical shape of microspheres could be formed successfully with the composition of 15 wt% of PES, 5 wt% of PEG and 80 wt% of NMP solvent using phase inversion in a distilled water coagulation bath.

When using magnifications of 200 \times , 370 \times , and 1,000 \times , the tiny pores on the outer surface of the PES microcapsule can be observed clearly as shown in Figure 4.2 (a-c). These pores played an important role in enhancing the specific surface area for the Ni ion to reach the active sites in the adsorption process.

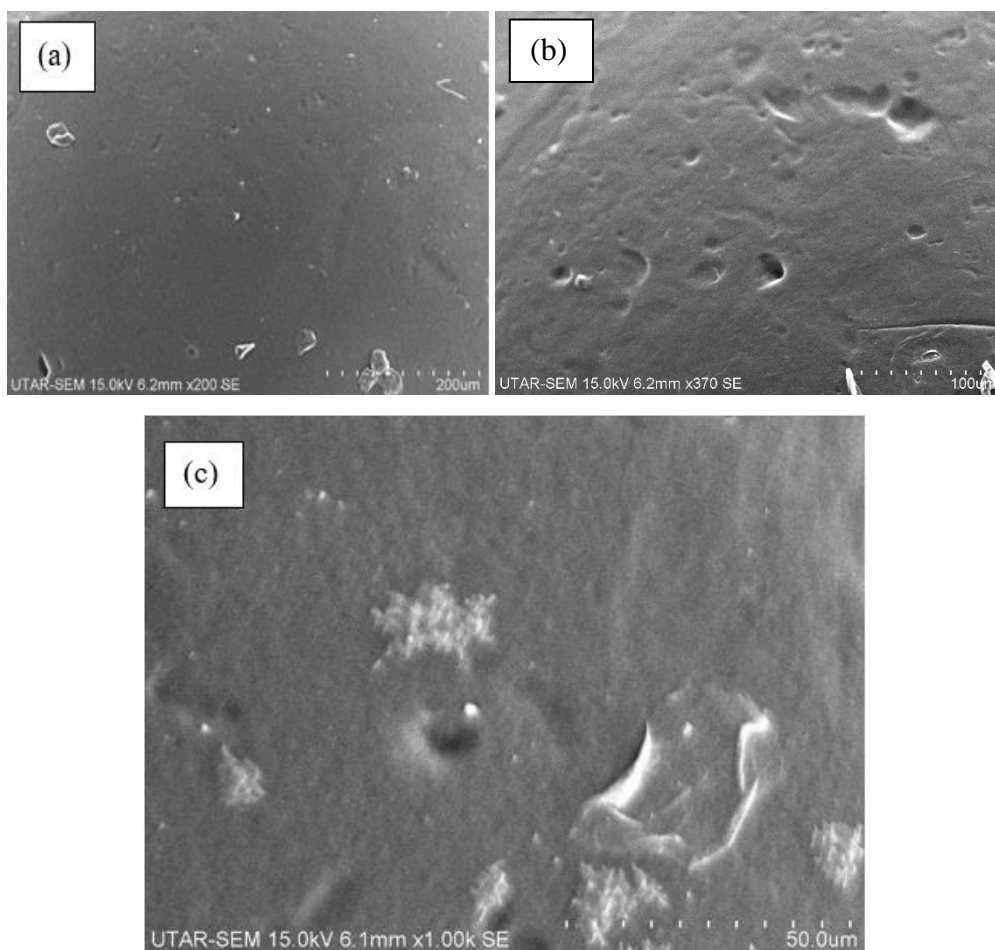


Figure 4.2: SEM Outer Surface Images of PES Microsphere at (a) 200 \times Magnification (b) 370 \times Magnification (c) 1,000 \times Magnification

Furthermore, the cross-sectional surface of PES microcapsule was observed by slowly cutting the microcapsule as shown in Figure 4.3 (a-b) with the magnification of $60\times$ and $120\times$. From Figure 4.3 (a), it can be observed that there were a few large pores in the center of the microspheres, and these pores will influence the adsorption capacity and internal surface area. Additionally, the outer part cross-sections looked like a porous structure with straight microchannels and a hollow central part. These straight microchannels and finger-like cavities could be observed clearly in Figure 4.3 (b). According to Guillen et al. (2011), the formation of finger-like cavities was due to the instantaneous demixing that occurred during phase inversion, indicating that PES microspheres were formed very rapidly after immersion in the coagulant bath. Due to this demixing process, the highly porous substructure, which consists of finger-like cavities and finely porous and thin skin layers, could be observed in PES microspheres.

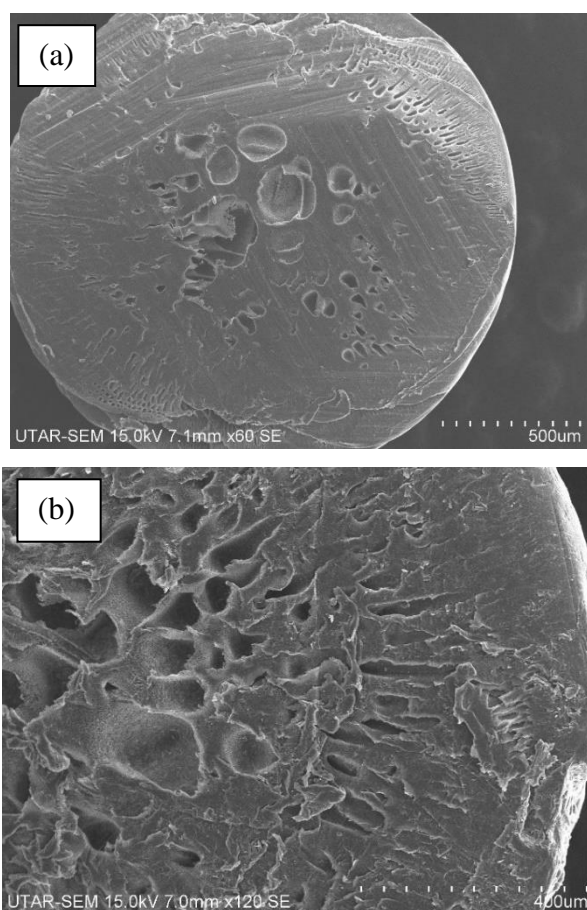


Figure 4.3: SEM Cross Sections Images of PES Microcapsule at (a) $60\times$ Magnification and (b) $120\times$ Magnification

Figure 4.4 (a) illustrates a further magnification of the surface of the porous structure. According to Lakshmi et al. (2012), due to the hollow porous structure, it could provide a larger surface area to immobilize heavy metal ions inside microspheres. The straight microchannels could enhance the mass transfer phenomena during adsorption. When the straight microchannels and the hollow porous structure were magnified as shown in Figure 4.4 (b-c), PES microspheres showed a complete and uniformly distributed porous structure.

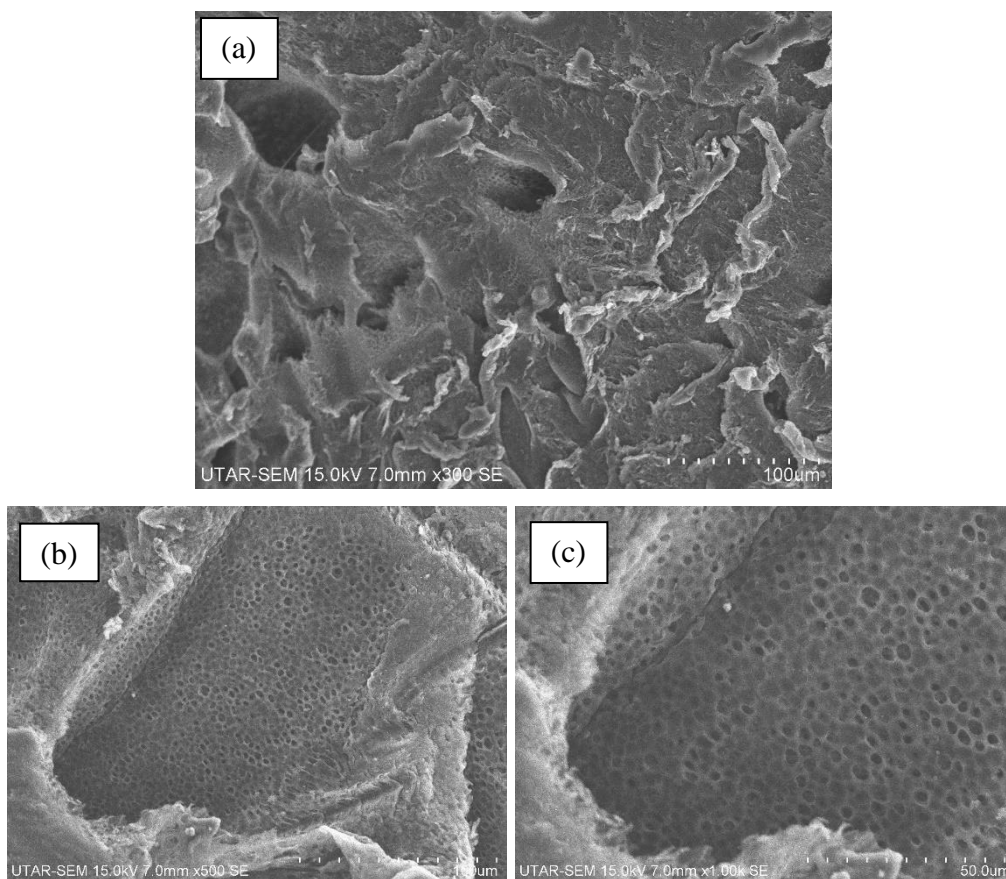


Figure 4.4: SEM Cross Sections Images of PES Microsphere at (a) 300× Magnification (b) 500× Magnification (c) 1,000× Magnification

In addition, EDX analysis was performed to study the elemental compositions of PES microcapsules before adsorption. Figures 4.5 demonstrate the EDX results of PES microcapsules before adsorption. Basically, PES microspheres consist of carbon (C), oxygen (O), and sulfur (S). The weight percentages of C, O, and S before adsorption were found to be 63.15%, 31.72%, and 5.13%, respectively. The presence of these elements matches the structure of PES polymer.

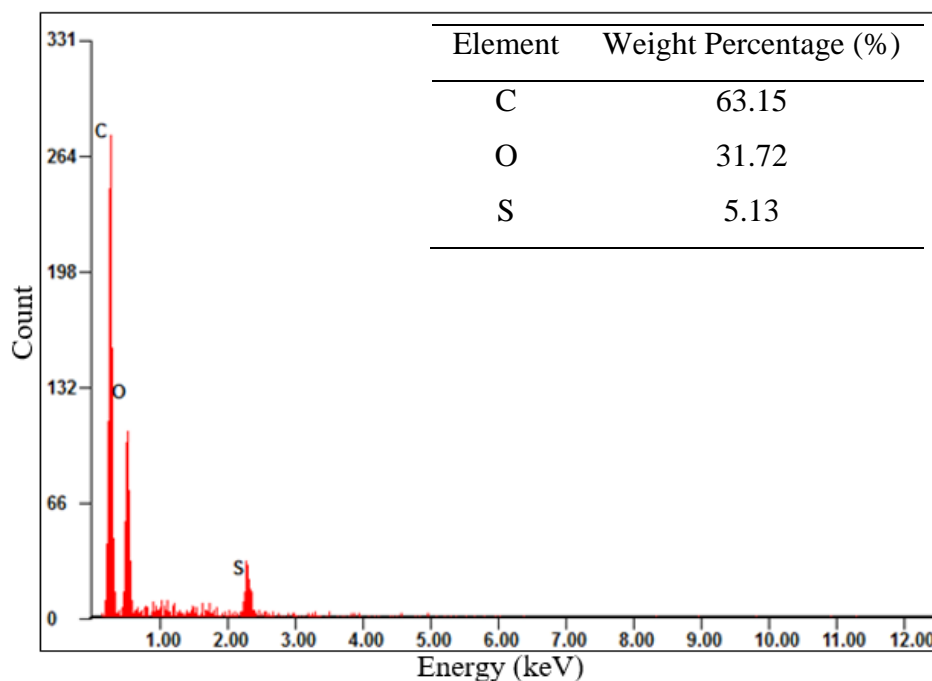


Figure 4.5: EDX Results of PES Microcapsules Before Adsorption

4.1.2 FTIR

FTIR was applied to analyse and determine the functional group that exists in the PES microcapsule. From the results, the graph of transmittance percentage against wavenumber was plotted and shown in Figure 4.6. The peaks were identified and compared with the journal article to determine the functional group.

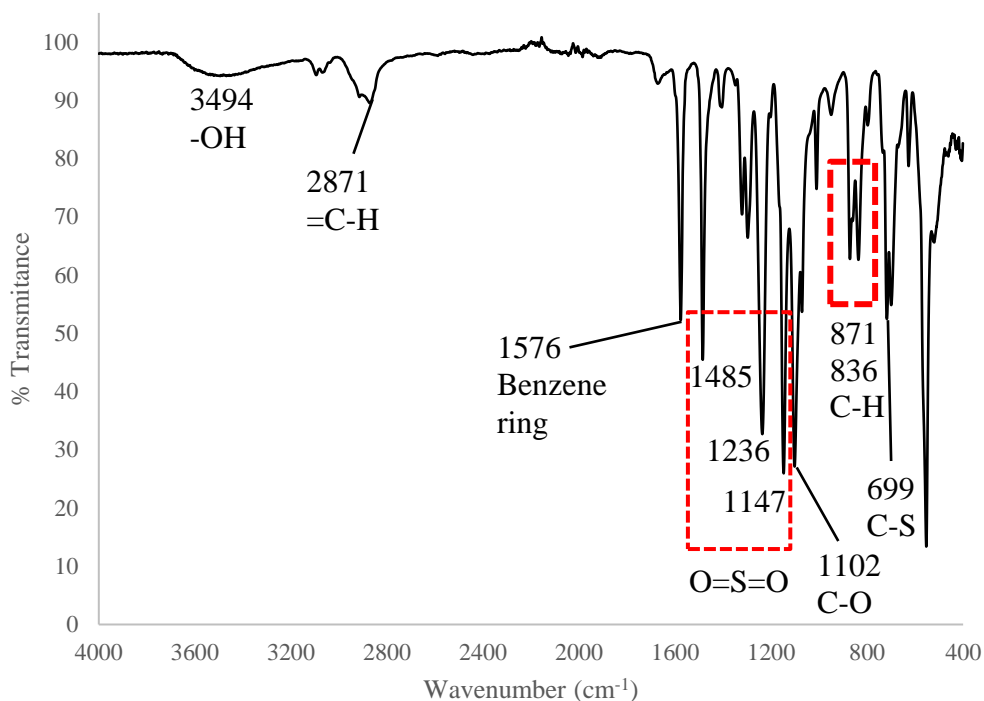


Figure 4.6: FTIR Spectra of PES Microcapsule

First of all, a broad band at 3494 cm⁻¹ was observed because of the OH-bending of hydroxyl group. It might be due to the presence of moisture on the surface and adsorbed water molecules in the PES microcapsule. The stretching vibrations of the =C-H groups at 2871 cm⁻¹ were observed and proven to indicate the existence of 1,4-disubstituted benzene ring (Sandoval-Olvera et al., 2017). Also, the wavelength of 1576 cm⁻¹ corresponded to the stretching vibration of C=C bond, which confirmed the existence of the benzene ring. Moreover, the peaks located at 1485 cm⁻¹, 1236 cm⁻¹, and 1147 cm⁻¹ were the stretching vibration bands of a sulfonyl group. According to Sandoval-Olvera et al. (2017), the sulfonyl group stretching appeared at wavelength between 1250–1290 cm⁻¹ and 1165–1120 cm⁻¹. The next peak located at 1102

cm^{-1} corresponded to the C–O bond stretching, which normally was found between wavelengths of 1300 and 1000 cm^{-1} . The stretching vibrations of C–H stretch were observed at 871 and 836 cm^{-1} , and the intense absorption peak at 699 cm^{-1} was the vibration band of the C–S bond. Therefore, the presence of PES polymer was verified by significant absorption of the these peaks, including peaks of 1,4-disubstituted benzene ring (=C-H), benzene ring (C=C), sulfonyl group, C-O bond stretching, C-H bending, and C-S bending.

4.1.3 Surface Area Analysis: BET Analysis

The properties of PES microspheres that can affect their adsorption performance in heavy metal and dye removal, including BET specific surface area, total pore volume and average pore diameter were studied. The BET results of PES microspheres are shown in Table 4.1.

Table 4.1: Surface Area Analysis Results of PES Microcapsule

Surface Properties	Results
Specific Surface Area (m^2/g)	10.9710
Total Pore Volume (cm^3/g)	0.0147
Average Pore Diameter (nm)	5.3597

When compared with the literature, the BET surface area of the synthesized PES microcapsule, using 15 wt% of PES polymer and 5 wt% of the pore-forming agent PEG (10.9710 m^2/g) was actually higher than the PES microspheres produced by Lakshmi et al. (2012), using 10 wt% of PES polymer and 6 wt% of pore forming agent PVPK 17 (7.30 m^2/g). Another group of researchers reported that the average surface area of PES microspheres containing graphene oxide was 11.4 m^2/g (Gujar and Mohapatra, 2015). Thus, the BET specific surface area of PES microcapsule was comparable with results obtained from different papers. Besides, the total pore volume of PES microcapsule was 0.0147 cm^3/g and the average pore diameter was 5.3597 nm. Since the diameter of the pores was in the range of 2 to 50 nm, the microspheres can be categorized to be the mesoporous size material. According to Xia et al. (2019), MB has a parallelepiped shape with approximately 1.7 nm \times 0.76 nm \times 0.33 nm. Meanwhile, the metallic radius of Ni is 0.125 nm (Gonsalvesh et al.,

2016). Thus, these pollutants are small enough to be adsorbed in the pores of the PES microcapsule.

4.1.4 TGA

TGA analysis was conducted to study and determine the thermal stability and decomposition temperature of PES microspheres. The graph of weight loss (%) against temperature was plotted and shown in Figure 4.7. The curve was divided into three stages that illustrated the three zones of significant weight losses of PES microcapsules.

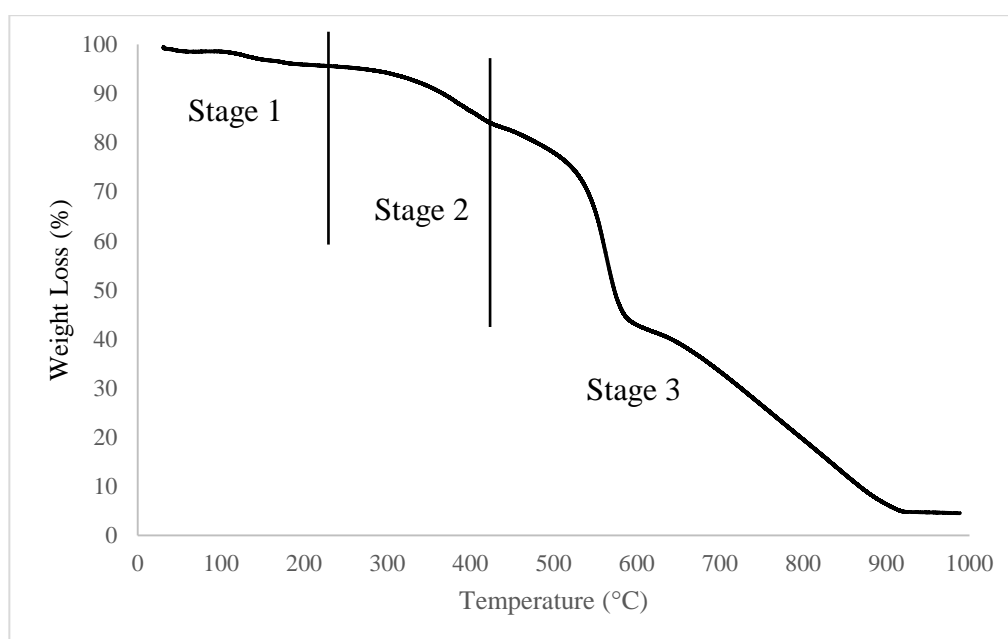


Figure 4.7: TGA Curve of PES Microcapsule

At Stage 1, which was the zone below the temperature of 210 °C, PES microspheres experienced the first slight weight loss in approximately the range of 100 to 180 °C, and the weight loss of Stage 1 was about 3.72 %. It was due to the loss of residual moisture, physisorbed compounds, and low volatile contaminants.

Furthermore, the weight of the PES microcapsule continued to decrease in Stage 2. The second significant weight loss occurred within a temperature range of approximately 300 to 420 °C, amounting to approximately 11.52%. According to Han et al. (2001), there was a 17% weight loss attributed to the evaporation of NMP solvent within a temperature range of 300 to 400 °C,

with significant decomposition of NMP solvent observed at 370 °C and above. Thus, the results align with the literature, demonstrating that the weight loss was primarily due to the evaporation of NMP solvent trapped in the PES microcapsules, with significant decomposition of NMP solvent occurring at 360 °C and above as shown in Figure 4.7.

Next, PES microspheres experienced a third weight loss at Stage 3, which was the zone above 420 °C. At the temperature range of 460 to 560 °C, significant weight loss can be observed. The weight loss of about 40.05 % for all the microcapsules at about 560 °C was due to the thermal degradation of PES polymer in the microspheres. According to Farnam, Mukhtar and Shariff (2016), PES polymer decomposed at temperatures between 450 and 550 °C. Thus, the temperature was slightly extended to 460 °C from the experiment with the highest weight loss observed at 570 °C. It indicated PES microspheres can withstand high temperatures and its decomposition temperature was 570 °C.

4.1.5 pH drift

The pH drift method was used to determine the pH of point of zero charge (pH_{PZC}) of PES microcapsules and evaluate their surface charge. The pH_{PZC} can be determined from the graph of final pH against initial pH, as shown in Figure 4.8. The dotted line represents the tie line, where the final pH is equal to the initial pH. From Figure 4.8, the intersection point between the two curves was found to be pH_{PZC} , which was determined to be pH 5.60. Thus, at pH 5.60, PES microcapsules have a net zero surface charge, indicating an equal amount of positive and negative charges on their surface. Below a pH of 5.60, the surface of PES microcapsules had a net positive charge. Conversely, at pH values above 5.60, the surface of PES microcapsules was negatively charged, favouring the adsorption of positively charged species.

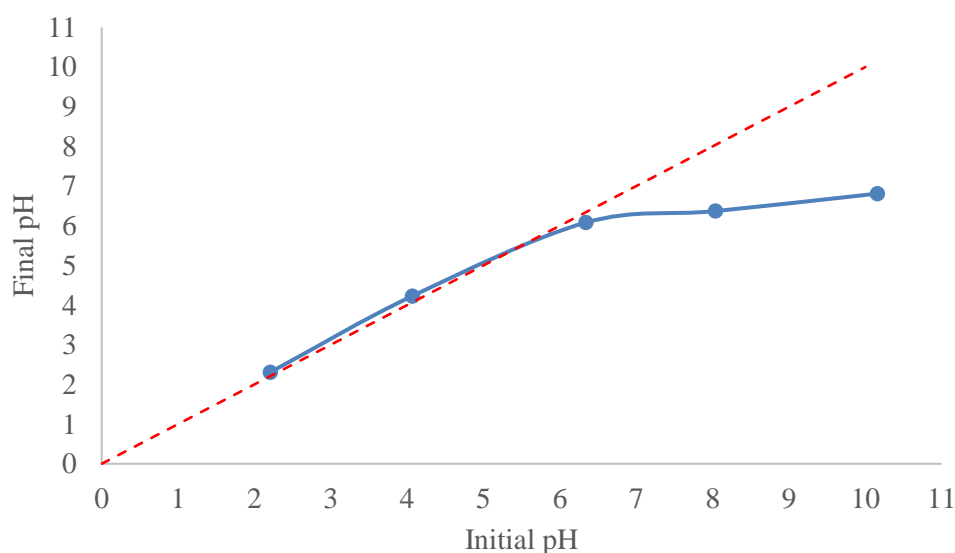


Figure 4.8: Point of Zero Charge Results of PES Microcapsule

From the pH drift method, PES microspheres at an initial pH of 10.16 were reduced to a final pH of 6.81, indicating that the surface charge of microcapsules was positive and adsorbed the negative hydroxide ions in the alkaline solution, causing a decrease in pH. On the other hand, PES microcapsules at an initial pH of 4.07 were increased to a final pH of 4.23, which indicated that the microcapsules were slightly negatively charged and adsorbed a small amount of positive hydronium ions from the acidic solution.

4.2 Statistical Analysis and Optimization Design Study of Ni Removal Efficiency

RSM using the CCD model was applied to study the interaction of different process parameters, including pH of the solution, microcapsule loading and initial concentration of Ni sample, and to analyse how the parameters can affect the removal efficiency of Ni. The optimization design study was to find the optimum operating parameter values that can maximize the removal efficiency.

4.2.1 Regression Analysis of Ni Removal

Table 4.2 showed the removal efficiency of Ni in response to the combination of three independent variables, which were pH (X_1), microcapsule loading (X_2), and initial concentration of Ni (X_3). The response variable was removal efficiency (%).

Based on Design Expert software, the model suggested was a quadratic model as it had the highest R-squared (R^2) value and a lack of fit p-value less than 0.0001, which indicated that the model is best fitted and significant. Thus, the quadratic model for Ni adsorption efficiency was significant and the removal efficiency response equation was shown in Equation 4.1 below.

Ni Removal Efficiency (%)

$$\begin{aligned}
 &= 144434.28 - 3873.897X_1 - 960.462X_2 - 2.886X_3 \\
 &+ 257.020X_1X_2 + 0.7700X_1X_3 - 0.1731X_2X_3 + 257.976X_1^2 \\
 &+ 16.199X_2^2 + 0.0793X_3^2 - 17.108X_1^2X_2 - 4.316X_1X_2^2 \\
 &+ 0.2869X_1^2X_2^2
 \end{aligned}$$

(4.1)

Table 4.2: Ni Removal Efficiency Based on CCD Experimental Design Matrix

Run	Independent Variables			Removal Efficiency (%)	
	X_1 : pH	X_2 : Microcapsule loading (g/L)	X_3 : Initial Ni Concentration (mg/L)	Experimental Values	Predicted Values
1	8	20	15	0.00	0.00
2	8	30	15	5.69	1.19
3	8	30	15	0.00	1.19
4	10	35	20	92.92	92.65
5	8	30	25	15.05	13.60
6	8	30	15	0.00	1.19
7	10	25	20	91.95	94.54
8	6	25	20	0.00	0.00
9	10	35	10	79.43	81.39
10	8	30	5	2.71	4.58
11	12	30	15	98.94	99.48
12	10	25	10	68.55	65.98
13	4	30	15	0.00	0.05

Table 4.2 (Continued)

Run	Independent Variables			Removal Efficiency (%)	
	X_1 : pH	X_2 : Microcapsule loading (g/L)	X_3 : Initial Ni Concentration (mg/L)	Experimental Values	Predicted Values
14	6	25	10	0	1.10
15	8	30	15	0	1.19
16	8	30	15	0	1.19
17	6	35	20	0	2.89
18	8	30	15	0	1.19
19	8	40	15	9.38	10.32
20	6	35	10	24.71	22.44

For the analysis of variance (ANOVA), Table 4.3 showed the results of ANOVA generated and calculated from Design Expert software according to the experimental values. The analysis was to identify the significance and reliability of the model. F-value and p-value from Table 4.3 were used to determine the significance and effectiveness of the terms in the model. The F-value indicated the relationship of the variables within and across the model and determined the significance of the model. The p-value indicated the closeness of the predicted Ni removal efficiency to the experimental Ni removal efficiency. With an F-value of 243.93, the model is significant, indicating there is only 0.01% chance that it could be due to noise, and the p-value was less than 0.0001. These values proved that the model was significant. For terms in the model, p-values that are less than 0.05 suggest that the model terms are significant. Conversely, p-values greater than 0.10 suggest that the model terms are insignificant. Therefore, for this case, there are eight terms that are significant model terms, which are X_1 , X_3 , X_1X_3 , X_2X_3 , X_1^2 , X_3^2 , $X_1X_2^2$, and $X_1^2X_2^2$. From the ANOVA table, it can also be observed that the pH (X_1) term had the largest value of F-value, which was 534.29, and it can be said that the term had the largest impact on this model.

Moreover, the lack of fit F-value of 3.44 indicates that the model's lack of fit was insignificant compared to the pure error. Moreover, there is only an 11.48% chance that this lack of fit F-value could be caused by noise and variation. In other words, it indicated that the model terms were best fitted with the model.

Table 4.3: ANOVA Table for Ni Removal Efficiency

Source	Sum of Squares	Degree of Freedom	Mean Square	F-value	p-value	
Model	26814.75	12	2234.56	243.93	< 0.0001	Significant
X_1 – pH	4894.56	1	4894.56	534.29	< 0.0001	Significant
X_2 – Microcapsule Loading (g/L)	43.99	1	43.99	4.80	0.0645	
X_3 – Initial Concentration of Ni (mg/L)	84.92	1	84.92	9.27	0.0187	Significant
$X_1 X_2$	20.67	1	20.67	2.26	0.1767	
$X_1 X_3$	474.32	1	474.32	51.78	0.0002	Significant
$X_2 X_3$	149.82	1	149.82	16.35	0.0049	Significant
X_1^2	3531.53	1	3531.53	385.50	< 0.0001	Significant
X_2^2	21.0	1	21.00	2.29	0.1738	
X_3^2	94.37	1	94.37	10.30	0.0149	Significant
$X_1^2 X_2$	19.80	1	19.80	2.16	0.1850	
$X_1 X_2^2$	759.83	1	759.83	82.94	< 0.0001	Significant
$X_1^2 X_2^2$	3593.76	1	3593.76	392.30	< 0.0001	Significant

Table 4.3 (Continued)

Source	Sum of Squares	Degree of Freedom	Mean Square	F-value	p-value	
Residual	64.13	7	9.16			
Lack of Fit	37.15	2	18.57	3.44	0.1148	Not Significant
Pure Error	26.98	5	5.40			
Corrected Total	26878.88	19				

For the regression model analysis, the results are shown in Table 4.4. The regression model was used to identify the precision of the experimental data, and the R-squared (R^2) ranged from 0 to 1. From the experimental results, the value of R^2 was 0.9976, and it indicated that 99.76 % of the data could fit the model well and the model had a high precision. Besides, the adjusted R^2 of 0.9935 implied that the correlation was 99.35 % reliable when there was an increase of significant terms in the model. When there is an increase of significant terms in the model, the higher the adjusted R^2 can be obtained and improve the fitness of the model. For adequate precision that measured the signal-to-noise ratio, the ratio of 40.984 was larger than 4, and it indicated that the model had an adequate signal that could be used to navigate the design space. Moreover, the standard deviation for the model was low, which is 3.03.

Table 4.4: Results for Fit Statistics Table

Fit Statistics	Values
Standard Deviation	3.03
Mean	24.47
Coefficient of Variation (%)	12.37
R-squared (R^2)	0.9976
Adjusted R^2	0.9935
Adequate Precision	40.9840

Figure 4.9 below shows the predicted and actual values derived from the model's correlation for the response. It was observed that the predicted values were closer to the experimental values for the Ni removal efficiency. So, the suggested model can be applied to predict the Ni removal efficiency within the studied range of pH, microcapsule loading and initial concentration of Ni.

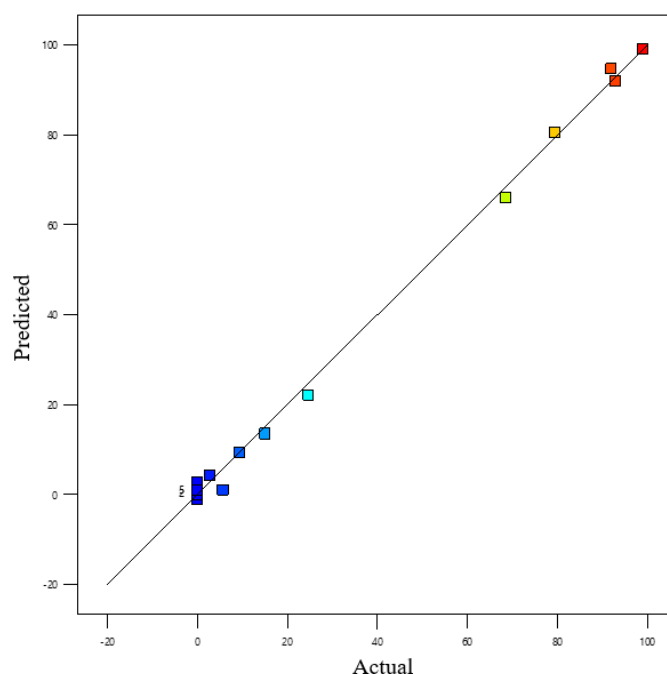


Figure 4.9: Predicted and Actual Values for Ni Removal Efficiency Response

4.2.2 Effect of Process Parameters on Ni Removal Efficiency

In this section, the effects of single process parameters on Ni removal efficiency were discussed with the RSM plots. As discussed above, the process parameters, pH (X_1) and initial concentration of Ni (X_3), were discovered to significantly affect the Ni removal efficiency.

Firstly, the parameter with the highest F-value and the greatest influence on removal efficiency was pH. Figure 4.10 illustrated the individual effect of pH on Ni removal efficiency. It can be observed from the graph that removal efficiency increased with higher pH. At a pH greater than 8, higher adsorption efficiency could be achieved. Experimental data showed that 98.94% of the maximum Ni ion removal was achieved at a pH of 12. The pH influenced the dissociation of acid-base groups on the surface of the PES microcapsule (De

Tuesta et al., 2022). This can be explained by the increasing total net negative charges on the surface of the PES microcapsule, which intensified electrostatic forces in the adsorption process as the pH of solution increased. Since Ni (II) ions are cations, the increasing total number of negative groups available for the Ni ions to bind decreases the competition between hydronium cations and Ni ions, leading to more Ni ions being electrostatically attracted to the PES microspheres and thus increasing removal efficiency. As the pH increased, the concentration of hydronium ions decreased, and the active sites on the surface of the adsorbent became dissociated forms that can exchange hydronium ions with Ni ions in the solution (De Tuesta et al., 2022). According to Rozaini et al. (2010), the highest removal efficiency of Ni can be achieved at a pH of 10. Thus, it has been proven that a higher pH can improve the removal efficiency of Ni metal ions in the adsorption process.

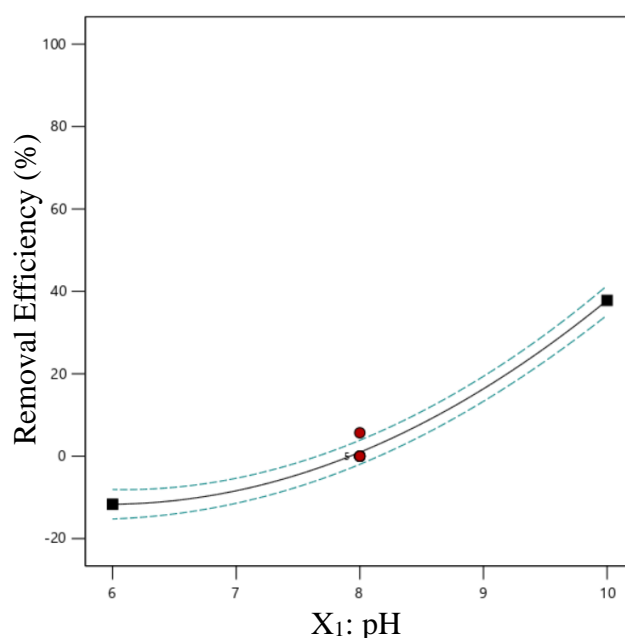


Figure 4.10: Graph of Individual Effect of pH on Ni Removal Efficiency

Furthermore, the initial concentration of Ni also influenced the adsorption efficiency. Graph of individual effect of initial concentration of Ni on Ni removal efficiency was shown in Figure 4.11. The graph demonstrated an increasing trend, indicating that a higher initial concentration could result in higher removal efficiency. This can be explained by the fact that an increase in the initial Ni concentration caused a higher concentration gradient in the low

range of Ni concentration. The high concentration gradient acted as the driving force to increase the equilibrium adsorption until the saturation of the adsorbent was reached. This increasing trend is supported by the research conducted by Alabsi, AL-Hamadi, and Alwesabi (2020), which also studied the removal of low concentration Ni ions in the range of 10 mg/L to 20 mg/L. At pH 8, it was found that an initial concentration of 20 mg/L had the highest removal efficiency of 90%, while the Ni removal efficiency at an initial concentration of 10 mg/L dropped tremendously to only 55%.

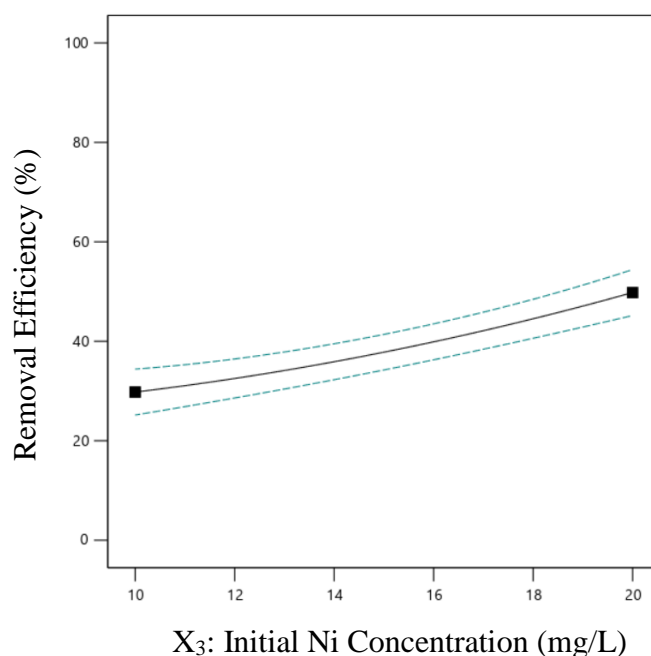


Figure 4.11: Graph of Individual Effect of Initial Concentration of Ni on Ni Removal Efficiency

For interaction between parameters, the terms X_1X_3 , X_2X_3 , and X_1X_2 ($X_1X_2^2$ and $X_1^2X_2^2$) are significant terms. Both interactions can affect the removal efficiency significantly. The first interaction term is X_1X_3 , which is the interaction between pH and initial concentration of Ni. Figure 4.12 (a) and (b) illustrated the three-dimensional surface plot and contour plot for the interaction between pH and initial concentration at the 95 % confidence level. At constant microcapsule loading of 30 g/L, it can be observed that the removal efficiency of Ni is increased when the pH is increased to 10 and the initial concentration of Ni is increased to 20 mg/L. As the initial concentration of Ni increased from 10 to 20 mg/L and the pH increased from 6 to 10, the removal efficiency

gradually increased and reached a maximum of 49 % at pH 10, and an initial concentration of 20 mg/L. Also, it can be observed that this interaction term gave a synergistic effect to the predicted response model and increased the removal efficiency.

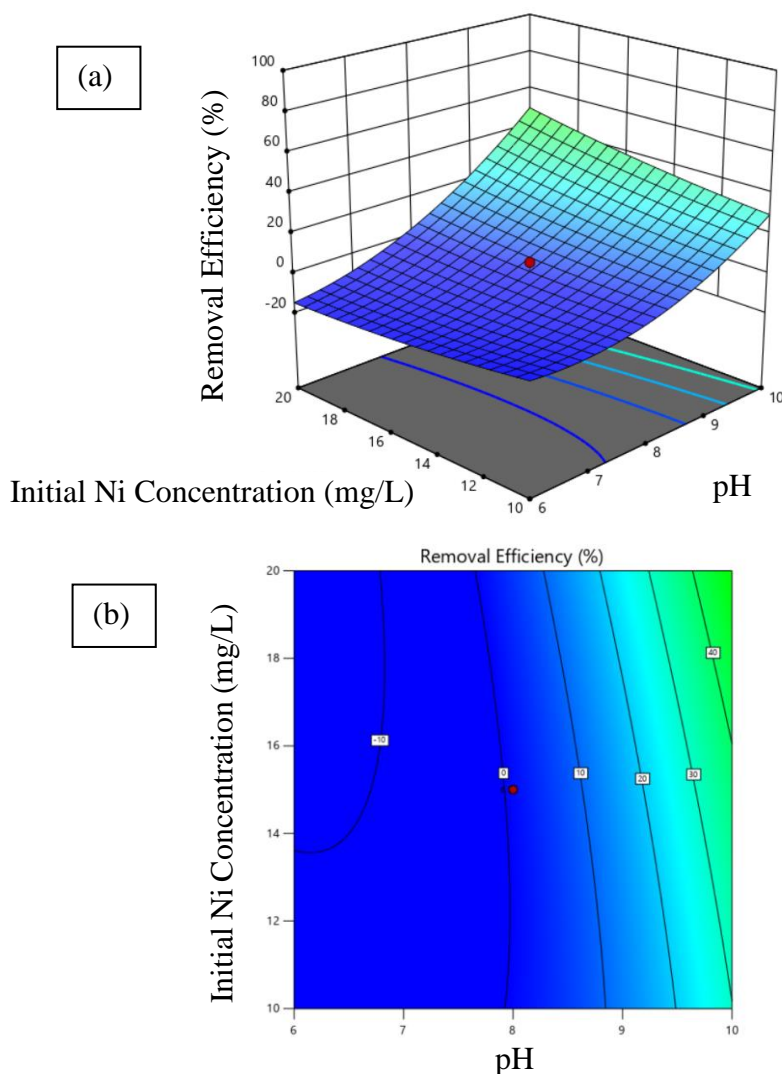


Figure 4.12: Interaction Effect between pH and Initial Ni Concentration on Removal Efficiency shown as (a) a Three-dimensional Surface Plot (b) a Contour Plot

Furthermore, the next significant interaction term is X_2X_3 , which is the interaction between microcapsule loading and initial concentration of Ni. Figure 4.13 (a) and (b) illustrated the three-dimensional surface plot and contour plot for the interaction between microcapsule loading and initial Ni concentration. At constant pH, it can be seen that the removal efficiency initially decreased and

then increased with the rise in microcapsule loading from 25 to 35 g/L. The lowest removal efficiency is 29.79 %, which occurred at microcapsule loading of 30 mg/L and initial concentration of 10 mg/L. On the other hand, the Ni removal efficiencies of 91.85 % can be obtained with a microcapsule loading of 35 g/L and initial concentration of 20 g/L, and removal efficiency decreased when the initial concentration decreased to 10 g/L with the same microcapsule loading of 35 g/L. Since this interaction contributed a minor antagonistic effect to the removal efficiency, it indicated this term is a low-level interaction to cause a decrease in removal efficiency. Due to the initial concentration range studied was low, the effect of microcapsule loading was insignificant, and the adsorption sites on the adsorbent remained unsaturated for the adsorption of Ni.

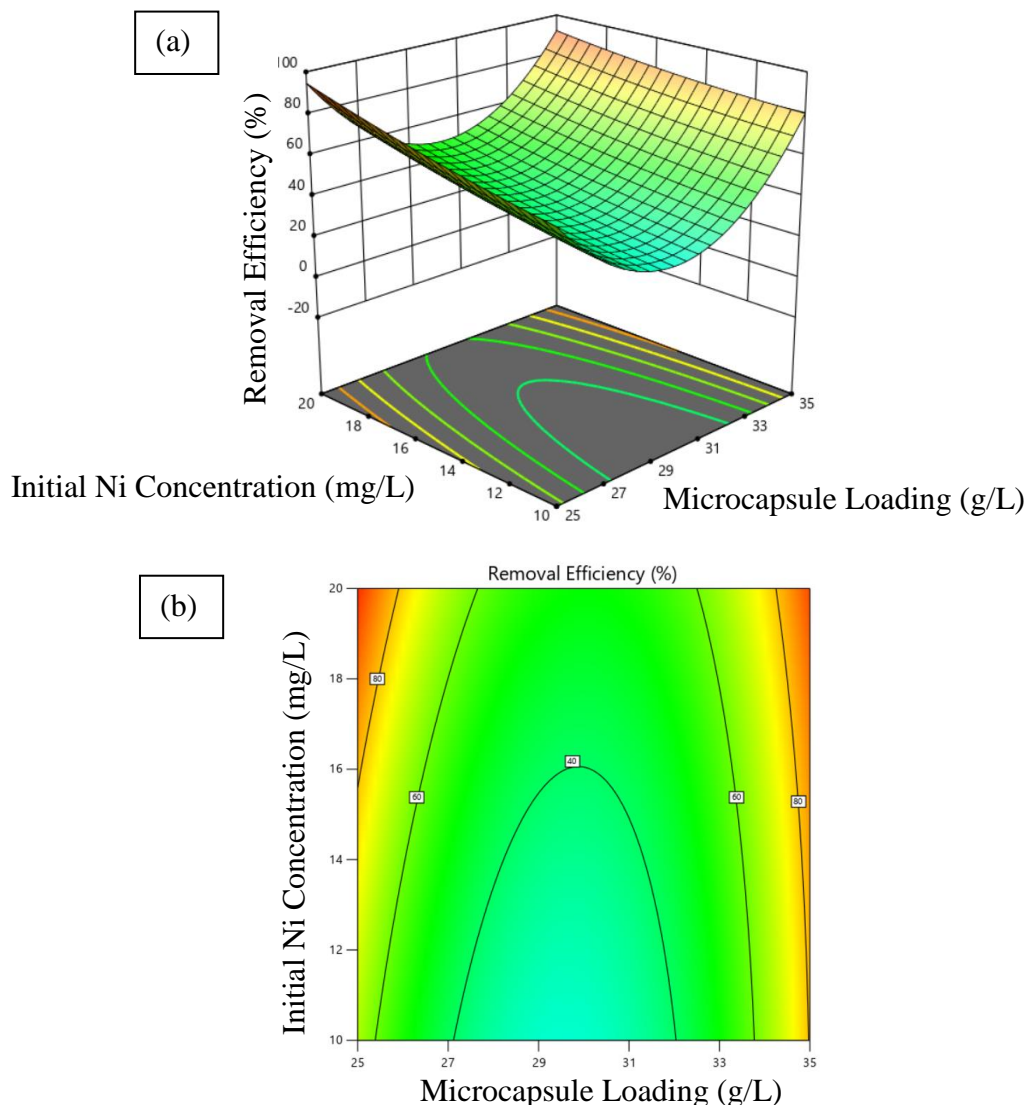


Figure 4.13: Interaction Effect between Microcapsule Loading and Initial Ni Concentration on Removal Efficiency shown as (a) a Three-dimensional Surface Plot (b) a Contour Plot

Moreover, the interaction term of X_1X_2 ($X_1X_2^2$ and $X_1^2X_2^2$) is also the significant term, which is the interaction between pH and microcapsule loading. Figure 4.14 (a) and (b) demonstrated the three-dimensional surface plot and contour plot for the interaction between microcapsule loading and pH at the 95 % confidence level. The peak Ni removal efficiency of 82.73 % occurred at pH 10 and microcapsule loading of 35 g/L, which was attributed to the $\pi - \pi$ interactions and cationic- π electron bonds between PES microcapsule and Ni molecules. With increasing pH, the Ni removal efficiency increased to 81.56 % at the microcapsule loading of 35 g/L. The interaction curves demonstrated that

the variation in microcapsule loading did not alter the overall trend, although the removal efficiency could be improved. The $X_1^2X_2^2$ interaction contributed a minor synergistic effect to the removal efficiency, it indicated this term is a low-level interaction to cause an increase in removal efficiency. The $X_1X_2^2$ interaction caused an antagonistic effect to the removal efficiency.

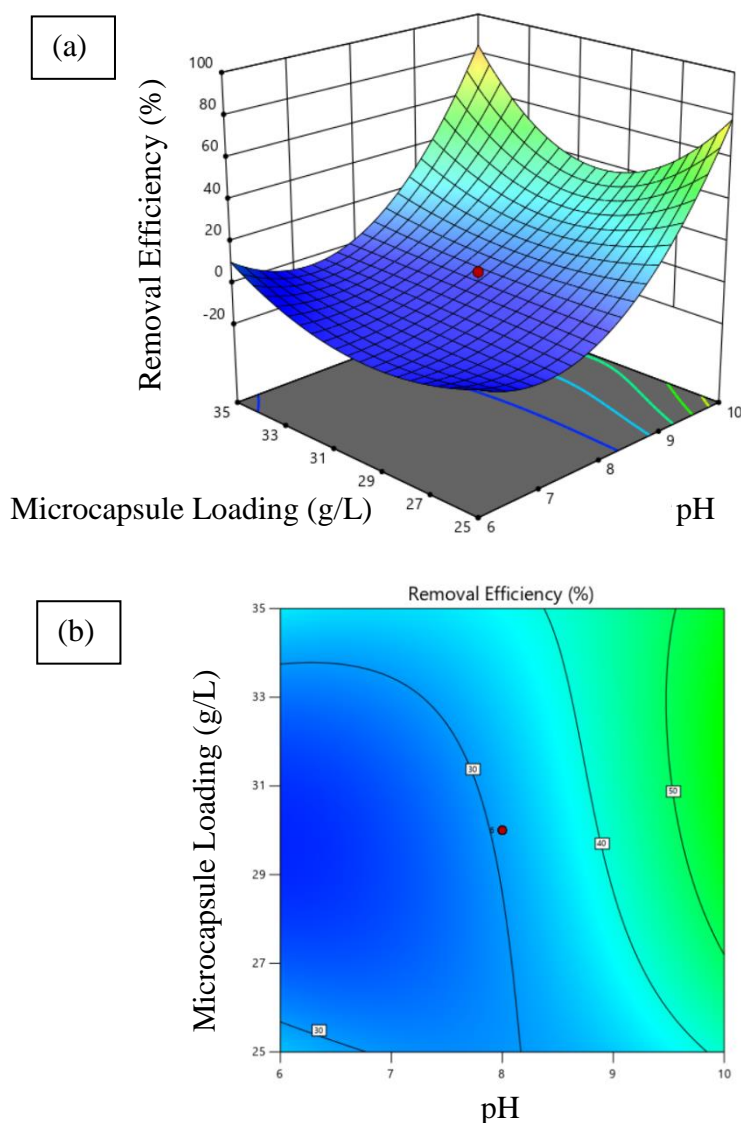


Figure 4.14: Interaction Effect between pH and Microcapsule Loading on Removal Efficiency shown as (a) a Three-dimensional Surface Plot (b) a Contour Plot

4.2.3 Optimization and Model Validation

Process optimization and model validation were conducted to optimize the process parameters to obtain maximum removal efficiency using Design Expert. Table 4.5 below showed the limits of each process parameter for optimization.

Table 4.5: Constraints Used to Optimize Ni Removal Efficiency

Variable	Goal	Lower Limit	Upper Limit
X_1 : pH	In Range	6	10
X_2 : Microcapsule Loading (g/L)	In Range	25	35
X_3 : Initial Ni Concentration (mg/L)	In Range	10	20
Y : Removal Efficiency (%)	Maximize	0.00	98.94

Design Expert predicted that an optimum removal efficiency of 93.98 % can be obtained with the following process parameters; pH of solution of 10, microcapsule loading of 25.0 g/L, and initial Ni concentration of 20 mg/L. For the optimized data sets given by the numerical modelling under optimum conditions, the confirmatory experiments were carried out by repeating three experimental runs using the suggested optimum condition to verify the predicted maximum removal efficiency of Ni. Table 4.6 showed the optimum process parameters suggested by the software, predicted removal efficiency, experimental removal efficiency and the deviation between predicted and experimental values.

The repeated experiments were found to give removal efficiencies of 88.94 %, 94.92 %, and 94.65 %, with a deviation of less than 10 %, which indicated that the predicted values were close to the experimental values. It was proven that the predicted optimum process parameters are valid. The optimum Ni removal efficiency achieved was 94.92 % at a pH of 9.99, microcapsule loading of 25.16 g/L and initial Ni concentration of 20.00 mg/L.

Table 4.6: Experimental and Predicted Removal Efficiency of Ni After Optimization

Solution No.	X_1: pH	X_2: Microcapsule Loading (g/L)	X_3: Initial Ni Concentration(mg/L)	Predicted Removal Efficiency (%)	Experimental Removal Efficiency (%)	Deviation (%)
1	9.78	25.00	19.97	81.41	88.94	9.24
2	9.98	25.16	20.00	90.82	94.92	4.51
3	10.00	25.00	19.83	93.98	94.65	0.72

4.3 Statistical Analysis and Optimization Design Study of MB Removal Efficiency

Similarly, CCD was used to study the interaction between each process parameter that can affect dye adsorption efficiency, including the pH of the solution, microcapsule loading and initial MB concentration. The studied range of initial concentration of MB was different from Ni removal, which was 1 to 5 mg/L. The optimization design study was conducted to find the optimum operating parameter values that can maximize MB removal efficiency.

4.3.1 Regression Analysis of MB Removal

Table 4.7 showed the removal efficiency of MB in response to the combination of three independent variables, which are pH (X_1), microcapsule loading (X_2), and initial MB concentration (X_3). The response variable was MB removal efficiency (%).

Based on Design Expert software, the model suggested was a quadratic model with the highest R-squared (R^2) value and a lack of fit p-value of less than 0.0001, which indicated that the model is best fitted and significant. Thus, the model for MB adsorption efficiency was significant, and the response equation was shown in Equation 4.2 below. The terms in the model were lesser than the terms in the Ni removal efficiency model.

$$\begin{aligned}
 &\text{MB Removal Efficiency (\%)} \\
 &= 1812.32 - 226.762X_1 - 112.906X_2 - 5.051X_3 \\
 &\quad + 13.371X_1X_2 + 1.944X_1^2 + 1.861X_2^2 \\
 &\quad - 0.2185X_1X_2^2
 \end{aligned}
 \tag{4.2}$$

Table 4.7: MB Removal Efficiency Based on CCD Experimental Design Matrix

Run	Independent Variables			Removal Efficiency (%)	
	X_1 : pH	X_2 : Microcapsule loading (g/L)	X_3 : Initial MB Concentration (mg/L)	Experimental Values	Predicted Values
1	6	25	4	30.67	28.28
2	8	40	3	47.66	50.77
3	10	35	4	55.26	50.14
4	8	30	5	18.36	20.94
5	10	35	2	59.53	60.24
6	4	30	3	25.09	26.86
7	6	35	4	32.31	31.48
8	8	30	3	38.06	31.05
9	8	20	3	33.46	33.93
10	10	25	4	35.58	36.50
11	6	25	2	37.98	38.38
12	6	35	2	45.18	41.58
13	8	30	3	29.85	31.05

Table 4.7 (Continued)

Run	Independent Variables			Removal Efficiency (%)	
	X_1 : pH	X_2 : Microcapsule loading (g/L)	X_3 : Initial MB Concentration (mg/L)	Experimental Values	Predicted Values
14	8	30	3	27.65	31.05
15	8	30	3	28.28	31.05
16	8	30	3	28.57	31.05
17	10	25	2	49.49	46.60
18	8	30	3	30.55	31.05
19	8	30	1	39.59	41.15
20	12	30	3	95.65	97.44

Table 4.8 showed the results of ANOVA generated from Design Expert software based on the experimental values. The F-value and p-value from Table 4.8 were used to determine the significance of the terms in the model. The F-value of 57.31 implied that the model is significant and there is only a 0.01 % chance that it could be caused by noise, and the p-value was less than 0.0001. These values proved that the model was significant and could be used to predict the MB removal efficiency. For the terms in the model, p-values that are less than 0.05 suggest that the model terms are significant. So, for this case, there are six terms that are significant model terms, which are X_1 , X_2 , X_3 , X_1^2 , X_2^2 , and $X_1X_2^2$. From the ANOVA table, it can also be observed that the pH (X_1) term had the largest value of F-value, which was 190.46, and it can be described that the term had the largest effect on this model. For Ni and MB removal, the pH of the solution played an important role in the adsorption, and it had the greatest impact on both models.

Moreover, the lack of fit F-value of 0.79 indicated that the lack of fit of the model was not significant compared to the pure error, with a 62.46% chance that this lack of fit F-value could be caused by noise. In other words, it indicated that the model terms were fitted with the model.

Table 4.8: ANOVA Table for MB Removal Efficiency

Source	Sum of Squares	Degree of Freedom	Mean Square	F-value	p-value	
Model	5243.58	7	749.08	57.31	< 0.0001	Significant
X_1 – pH	2489.36	1	2489.36	190.46	< 0.0001	Significant
X_2 – Microcapsule Loading (g/L)	280.23	1	280.23	21.44	0.0006	Significant
X_3 – Initial MB Concentration (mg/L)	408.24	1	408.24	31.23	0.0001	Significant
$X_1 X_2$	54.50	1	54.50	4.17	0.0638	
X_1^2	1593.27	1	1593.27	121.90	< 0.0001	Significant
X_2^2	210.02	1	210.02	16.07	0.0017	Significant
$X_1 X_2^2$	477.42	1	477.42	36.53	0.0002	Significant
Residual	156.85	12	13.07			
Lack of Fit	82.49	7	11.78	0.7925	0.6246	Not Significant
Pure Error	74.35	5	14.87			
Corrected Total	5400.43	19				

For the regression model analysis, the results were shown in Table 4.9. From the experimental results, the value of R^2 was 0.9710 and it indicated that 97.10 % of the data could fit the model well and the model had a high precision. Besides, the adjusted R^2 of 0.9540 implied that the correlation was 94.57 % reliable when there was an increase of significant terms in the model. The predicted R^2 of 0.7219 was slightly deviated from the adjusted R^2 , which was still used to predict the response. For adequate precision that measured the signal-to-noise ratio, the ratio of 33.4503 was larger than 4 and it indicated that the model had an adequate signal that could be used to navigate the design space. Moreover, the standard deviation for the model was low, which is 3.62.

Table 4.9: Results for Fit Statistics Table

Fit Statistics	Values
Standard Deviation	3.62
Mean	39.44
Coefficient of Variation (%)	9.17
R-squared (R^2)	0.9710
Adjusted R^2	0.9540
Predicted R^2	0.7219
Adequate Precision	33.4503

Figure 4.15 below shows the predicted and actual values derived from the model's correlation for the response. It was observed that the predicted values were close to the experimental values for the removal efficiency. So, the suggested model can be applied to predict the MB removal efficiency within the studied range of pH, microcapsule loading and initial MB concentration.

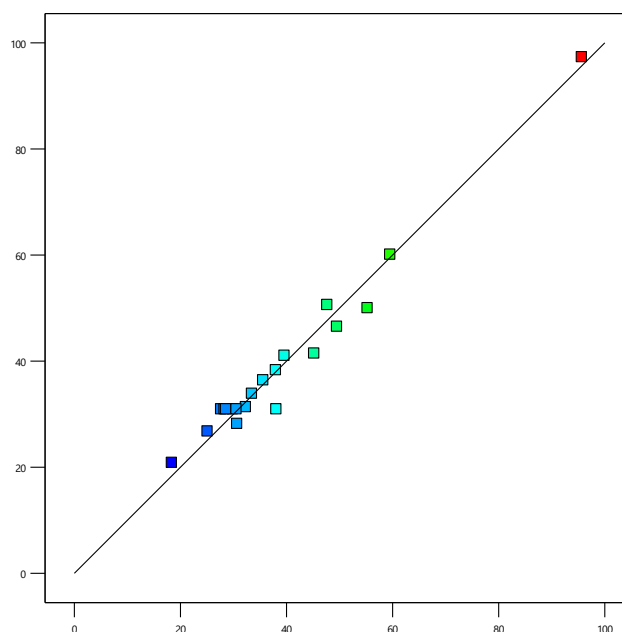


Figure 4.15: Predicted and Actual Values for MB Removal Efficiency Response

4.3.2 Effect of Process Parameters on MB Removal

For this section, the effects of single process parameters on MB removal efficiency were discussed with the RSM plots. All three process parameters, pH (X_1), microcapsule loading (X_2), and initial concentration of MB (X_3), were discovered to significantly affect the MB removal efficiency.

Firstly, the parameter that had the highest F-value and had the largest impact on the removal efficiency was pH. Graph of individual effect of pH on MB removal efficiency is shown in Figure 4.16. From the graph, it can be observed that the removal efficiency increased with higher pH, which is consistent with the trend observed for Ni removal efficiency. The highest adsorption efficiency could be achieved when the pH is increased to 12. As mentioned previously, the pH_{PZC} of the PES microspheres is 5.60, and the surface charge of the microspheres becomes negatively charged when the pH is

increased above 5.60. The increasing pH causes the deprotonation of the microsphere's surface and an increase in total net negative charges on the surface of the microspheres, which enhances the electrostatic interactions between MB and the microsphere's surface. MB is a cationic dye and carries an abundant cation, which can form a strong electrostatic attraction with the negative charges on the PES microcapsule. Under alkaline conditions, the competition between hydronium cations and MB cations is decreased, allowing more MB cations to be attracted electrostatically to the negatively charged PES microspheres, resulting in an increase in removal efficiency (Shi et al., 2020). Therefore, it has been proven that a higher pH of the solution can improve the removal efficiency of MB using PES microcapsules.

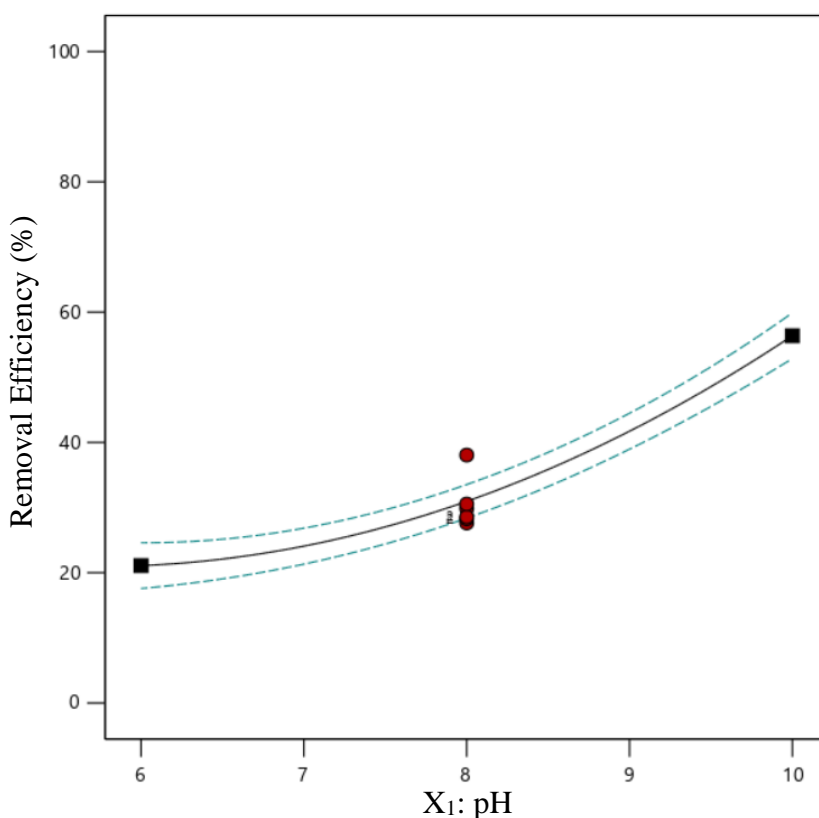


Figure 4.16: Graph of Individual Effect of pH on MB Removal Efficiency

The second parameter that can affect the removal efficiency of MB is microcapsule loading. Figure 4.17 illustrates the graph showing the individual effect of microcapsule loading on MB removal efficiency. From the graph, it can be observed that the removal efficiency increases slightly with an increase in microcapsule loading or adsorbent dosage. According to Oladoye et al. (2022), the increase in the amount of adsorbent results in an increase in the removal efficiency due to the increase in available active sites on the adsorbent and surface area for adsorption. At a microcapsule loading of 35 g/L, with a constant pH of 8 and an initial concentration of 3 mg/L, a higher surface area and active sites are provided for the adsorption of MB dye, leading to the maximum MB removal efficiency. The study shows that the available active sites of PES microspheres remained unsaturated for the MB adsorption due to the larger surface area of the adsorbent.

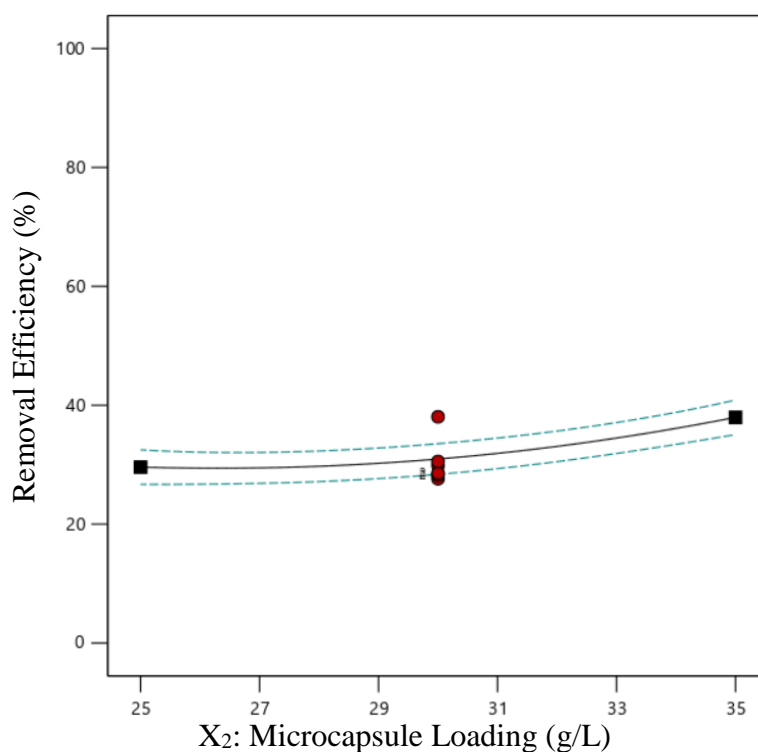


Figure 4.17: Graph of Individual Effect of Microcapsule Loading on MB Removal Efficiency

The last parameter that can influence the removal efficiency of MB was initial concentration of MB. Figure 4.18 demonstrated the graph of individual effect of initial MB concentration on MB removal efficiency. The graph shows that the removal efficiency decreased with an increase in the initial concentration of MB, which differs from the trend observed for Ni removal efficiency. According to Rápó and Tonk (2021), it could be due to the decrease in the available adsorption sites on the adsorbent surface. At low initial concentrations of MB, the number of adsorption binding sites is high, and MB molecules could be binded easily to the PES microspheres surface. At high initial concentrations, the total available adsorption sites are limited, and this might lead to a decrease in the removal efficiency of MB. The ratio of active sites to MB molecules is low, and not all molecules can be attracted and removed by the adsorbent (Rápó and Tonk, 2021). However, the adsorption capacity of the adsorbent was increased due to the high driving force from the mass transfer of MB at a high initial concentration of MB. The initial concentration of solute acts as a driving force for the adsorption, and increases the diffusion and mass transfer from the MB solution to the surface of the PES microcapsule (Oladoye et al., 2022).

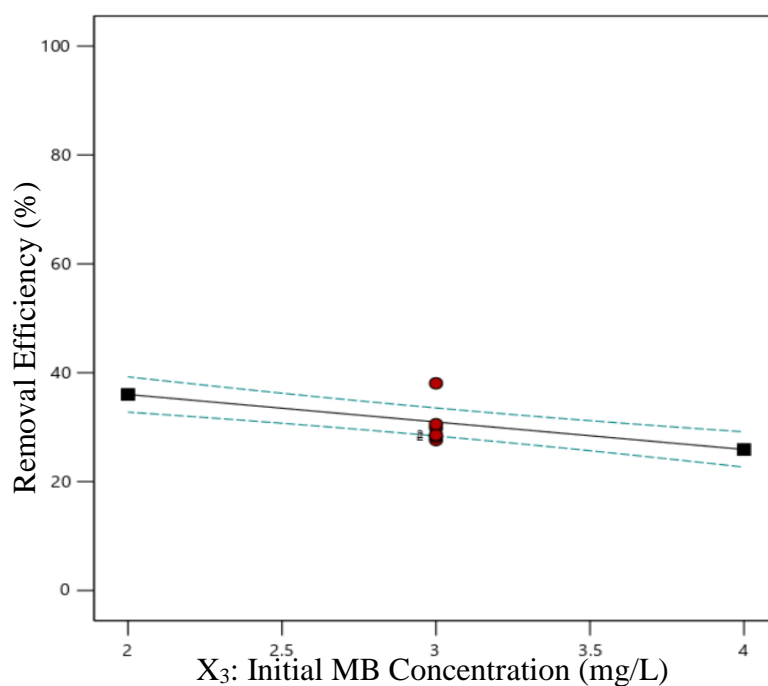


Figure 4.18: Graph of Individual Effect of Initial MB Concentration on MB Removal Efficiency

For interaction between parameters, the term X_1X_2 ($X_1X_2^2$) is the only significant term to affect MB removal efficiency, which is interaction between pH and microcapsule loading. Figure 4.19 (a) and (b) illustrated the three-dimensional surface plot and contour plot for the interaction between pH and microcapsule loading at the 95 % confidence level. The peak MB removal efficiency of 55.21 % occurred at pH 8, and microcapsule loading of 30 g/L from the interaction graph. With increasing pH and microcapsule loading, the MB removal efficiency increased from 32.42 % to 55.21 %. The $X_1X_2^2$ interaction contributed a minor antagonistic effect to the predicted removal efficiency, it indicated this term is a low-level interaction to cause a decrease in removal efficiency.

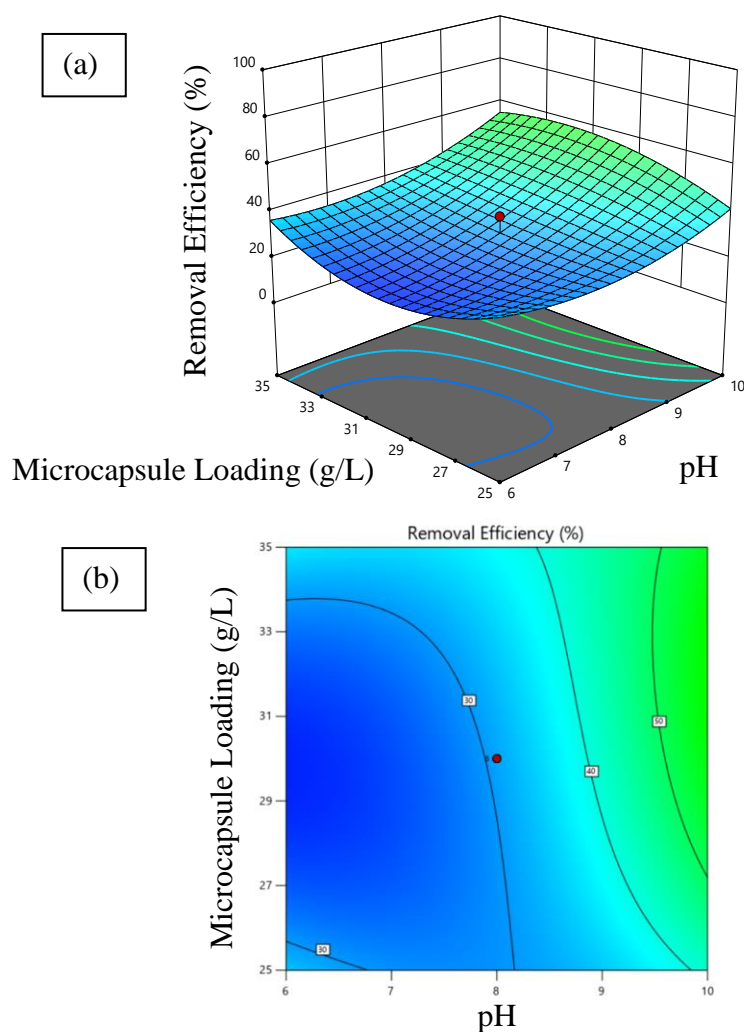


Figure 4.19: Interaction Effect between pH and Microcapsule Loading on MB Removal Efficiency shown as (a) a Three-dimensional Surface Plot (b) a Contour Plot

4.3.3 Optimization and Model Validation

Process optimization and model validation were conducted to optimize the process parameters to obtain maximum MB removal efficiency using Design Expert. Table 4.10 below showed the limits of each process parameter for optimization.

Table 4.10: Constraints Used to Optimize MB Removal Efficiency

Variable	Goal	Lower Limit	Upper Limit
X_1 : pH	In Range	6	12
X_2 : Microcapsule Loading (g/L)	In Range	25	35
X_3 : Initial MB Concentration(mg/L)	In Range	2	4
Y : Removal Efficiency (%)	Maximize	18.36	95.65

Design Expert software predicted that an optimum removal efficiency of 97.34 % can be obtained with the following process parameters; pH of solution of 12, microcapsule loading of 30.0 g/L, and initial concentration of MB of 3 mg/L. For the optimized data sets given by the numerical modelling under optimum conditions, the confirmatory experiments were carried out by repeating three experimental runs using the suggested optimum condition to verify the predicted maximum removal efficiency of MB. Table 4.11 showed the optimum process parameters suggested by the software, predicted removal efficiency, experimental removal efficiency and the deviation between predicted and experimental values.

The repeated experiments were found to give removal efficiencies of 94.97 %, 94.21 %, and 93.53 %, with a deviation of less than 5 %, which indicated that the predicted values were close to the experimental values. It was proven that the predicted optimum process parameters are valid. The optimum MB dye removal efficiency achieved was 94.97 % at a pH of 11.99, microcapsule loading of 33.00 g/L and initial concentration of Ni of 2.41 mg/L.

Table 4.11: Experimental and Predicted Removal Efficiency of MB After Optimization

Solution No.	X_1: pH	X_2: Microcapsule Loading (g/L)	X_3: Initial Concentration of Ni (mg/L)	Predicted Removal Efficiency (%)	Experimental Removal Efficiency (%)	Deviation (%)
1	11.99	33.00	2.41	98.17	94.97	3.26
2	11.81	32.18	2.22	96.78	94.21	2.66
3	11.93	29.18	2.71	97.95	93.53	4.51

4.4 EDX Analysis After Adsorption of Ni and MB

In addition, EDX analysis was performed on the cross-sectional surface of PES microcapsules after the adsorption of Ni (II) and MB. Figure 4.20 demonstrates the EDX results of PES microcapsules after Ni adsorption. After the adsorption of Ni, Ni element could be detected in the pores of PES microspheres. The weight percentage of Ni was found to be 0.31%. So, the presence of Ni proved the successful adsorption of Ni onto the pores of PES microcapsules.

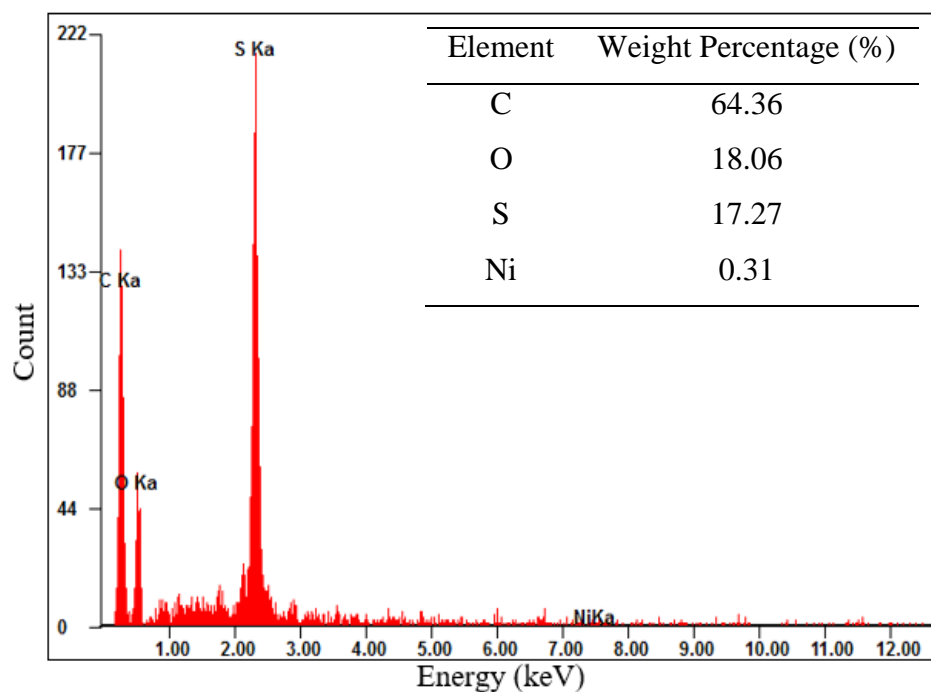


Figure 4.20: EDX Results of PES Microcapsules After Ni Adsorption

After the adsorption of MB dye, the cross-section of PES microcapsules was analysed. The chemical formula of MB is $C_{16}H_{18}ClN_3S$ and these elements were examined. The nitrogen (N) and chlorine (Cl) elements were detected in the pores, proving the presence of the MB dye in the pores. The weight percentages of N and Cl were found to be 3.99% and 1.83%, respectively. Therefore, the presence of N and Cl also proved the successful adsorption of MB onto the pores of PES microcapsules.

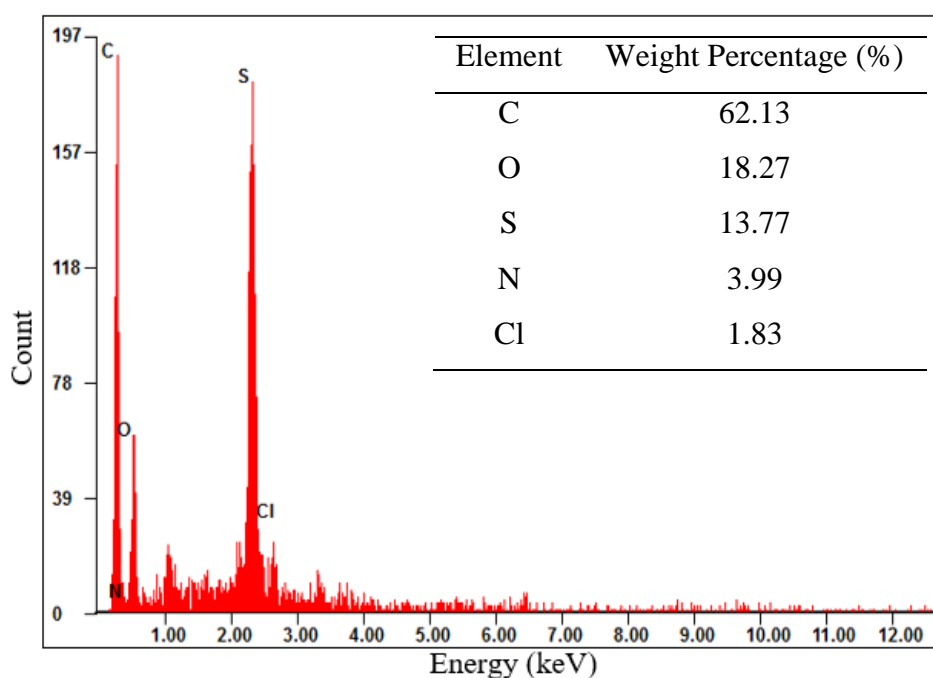


Figure 4.21: EDX Results of Microcapsules After MB Adsorption

CHAPTER 5

CONCLUSIONS AND RECOMMENDATIONS

5.1 Conclusions

In conclusion, PES microcapsules exhibited the potential to be used as a novel adsorbent to adsorb and remove Ni heavy metal and MB dye from aqueous solutions. Several characterization studies, including SEM-EDX, FTIR, BET, TGA, and pH drift, had proven the PES microcapsules to possess suitable characteristics for the removal of Ni and MB dye via adsorption. SEM analysis of the outer surface and cross-sectional surface of PES microcapsules portrayed smooth and highly porous microchannels and finger-like cavities. These hollow porous structures could provide a larger internal surface area and higher Ni and dye adsorption capacity.

Moreover, FTIR analysis verified the presence of PES polymer with significant absorption peaks. BET analysis was used to study the specific surface area and average pore diameter of the PES microcapsule, revealing that the microspheres are mesoporous-sized adsorbents. Subsequently, TGA results showed a three-stage thermal degradation of the PES microcapsule, with a decomposition temperature of 570 °C for PES microspheres. The last characterization study involved pH drift, and the pH_{PZC} was found to be 5.60. The surface charges of PES microcapsules were negative when the pH was increased above 5.60, favoring the adsorption of positively-charged pollutants.

The RSM was applied to optimize the process parameters, including pH, microcapsule loading, and initial concentration. The optimum Ni removal efficiency achieved was 94.92% at a pH of 9.98, microcapsule loading of 25.16 g/L, and initial Ni concentration of 20.00 mg/L. Meanwhile, the optimum MB dye removal efficiency achieved was 94.97 % at a pH of 11.99, microcapsule loading of 33.00 g/L, and initial MB concentration of 2.41 mg/L. The interactions between these parameters on the removal efficiency of Ni and MB dye were studied using response surface plots and contour plots. It was found that pH had the most significant impact on the removal efficiency of both Ni

and MB dye. The EDX analysis further proved the successful adsorption of Ni and MB dye onto the pores of PES microcapsules.

It can be concluded that PES microspheres are potential adsorbent to remove Ni and MB dye from aqueous solution as high removal efficiency could be achieved.

5.2 Recommendations for Future Work

Some recommendations could be carried out in the future work to improve its experimental quality and application in industries. The recommendations are listed as follows:

- (i) The synthesis method of PES microcapsules can be improved in future work so that the synthesis time for large quantities of PES microcapsules can be reduced.
- (ii) This study focussed on the lab-scale batch adsorption of Ni and MB dye. It is recommended that pilot-scale adsorption be implemented using the proposed optimum conditions to confirm the appropriateness of applying this wastewater treatment technique on an industrial scale.
- (iii) The internal surface area of the PES microcapsule can be improved and increased as the results obtained are relatively low compared to other research papers.
- (iv) The contact time can be investigated to reduce the retention time for the adsorption using PES microcapsule in the future work.
- (v) The reusability study of PES microcapsules can be studied in the future work.

REFERENCES

- Abbas, S. H., Ismail, I. M., Mostafa, T. M. and Sulaymon, A. H., 2014. Biosorption of heavy metals: a review. *Journal of Chemical Science and Technology*, 3(4), pp.74-102.
- Ahmad, A., Mohd-Setapar, S. H., Chuong, C. S., Khatoon, A., Wani, W. A., Kumar, R., and Rafatullah, M., 2015. Recent advances in new generation dye removal technologies: novel search for approaches to reprocess wastewater. *RSC advances*, 5(39), pp.30801-30818.
- Akpor, O. B., Ohiobor, G. O. and Olaolu, D. T., 2014. Heavy metal pollutants in wastewater effluents: sources, effects and remediation. *Advances in Bioscience and Bioengineering*, 2(4), pp.37-43.
- Aktar, S., Mia, S., Makino, T., Rahman, M. M., and Rajapaksha, A. U., 2023. Arsenic removal from aqueous solution: A comprehensive synthesis with meta-data. *Science of The Total Environment*, Volume 862, p.160821.
- Alabsi, B. I., AL-Hamadi, M. M. and Alwesabi, A. S., 2020. Preconcentration of trace nickel ions from aqueous solutions by using a new and low cost chelating polystyrene adsorbent. *Arabian Journal of Chemistry*, 13(9), pp.6986-6994.
- Ali, H., Khan, E. and Ilahi, I., 2019. Environmental chemistry and ecotoxicology of hazardous heavy metals: environmental persistence, toxicity, and bioaccumulation. *Journal of chemistry*.
- Azimi, A., Azari, A., Rezakazemi, M. and Ansarpour, M., 2017. Removal of heavy metals from industrial wastewaters: a review. *ChemBioEng Reviews*, 4(1), pp.37-59.
- Azmi, A. A., Jai, J., Zamanhuri, N. A. and Yahya, A., 2018. Precious metals recovery from electroplating wastewater: A review. *IOP Conference Series: Materials Science and Engineering*, Volume 358, p. 012024.
- Bankole, M. T., Abdulkareem, A. S., Mohammed, I. A., Ochigbo, S. S., Tijani, J. O., Abubakre, O. K. and Roos, W. D., 2019. Selected heavy metals removal from electroplating wastewater by purified and polyhydroxybutyrate functionalized carbon nanotubes adsorbents. *Scientific reports*, 9(1), p.4475.
- Barhoum, A. and García-Betancourt, M. L., 2018. Physicochemical characterization of nanomaterials: Size, morphology, optical, magnetic, and electrical properties. In: *Emerging applications of nanoparticles and architecture nanostructures*. s.l.:Elsevier, pp.279-304.
- Bhatia, D., Sharma, N. R., Singh, J. and Kanwar, R. S., 2017. Biological methods for textile dye removal from wastewater: A review. *Critical Reviews in Environmental Science and Technology*, 47(19), pp.1836-1876.

Carolin, C. F., Kumar, P. S., Saravanan, A., Joshiba, G. J., and Naushad, M., 2017. Efficient techniques for the removal of toxic heavy metals from aquatic environment: A review. *Journal of environmental chemical engineering*, 5(3), pp.2782-2799.

Chen, F., Luo, G., Yang, W. and Wang, Y., 2005. Preparation and Adsorption Ability of Polysulfone Microcapsules Containing Modified Chitosan Gel. *Tsinghua Science and Technology*, 10(5), pp.535-541.

Cossio, C., Norrman, J., McConville, J., Mercado, A., and Rauch, S., 2020. Indicators for sustainability assessment of small-scale wastewater treatment plants in low and lower-middle income countries. *Environmental and Sustainability Indicators*, Volume 6, p.100028.

da Silva Barbosa Ferreira, R., Florindo Salviano, A., Sonaly Lima Oliveira, S., Maria Araújo, E., da Nóbrega Medeiros, V., and de Lucena Lira, H., 2019. Treatment of Effluents from the Textile Industry through Polyethersulfone Membranes. *Water*, 11(12), p.2540.

De Beni, E., Giurlani, W., Fabbri, L., Emanuele, R., Santini, S., Sarti, C., Martellini, T., Piciollo, E., Cincinelli, A., Innocenti, M., 2022. Graphene-based nanomaterials in the electroplating industry: A suitable choice for heavy metal removal from wastewater. *Chemosphere*, Volume 232, p.133448.

De Tuesta, J. L. D., Roman, F. F., Marques, V. C., Silva, A. S., Silva, A. P., Bosco, T. C., Shinibekova, A. A., Aknur, S., Kalmakhanova, M. S. Massalimova, B. K., Arrobas, M., Silva, A. M. T., and Gomes, H. T., 2022. Performance and modeling of Ni (II) adsorption from low concentrated wastewater on carbon microspheres prepared from tangerine peels by FeCl₃-assisted hydrothermal carbonization. *Journal of Environmental Chemical Engineering*, 10(5), p.108143.

Department of Environment, 2009. *Environmental Quality (Industrial Effluent) Regulations* 2009. [Online] Available at: <https://www.doe.gov.my/wp-content/uploads/2021/08/Environmental_Quality_Industrial_Effluent_Regulations_2009_-_P.U.A_434-2009.pdf> [Accessed 12 July 2023].

Duraikkannu, S. L., Castro-Muñoz, R. and Figoli, A., 2021. A review on phase-inversion technique-based polymer microsphere fabrication. *Colloid and Interface Science Communications*, Volume 40, p.100329.

Ebnesajjad, S., 2011. Surface and material characterization techniques. In: *Handbook of adhesives and surface preparation*. s.l.:William Andrew Publishing, pp.31-48

Farnam, M., Mukhtar, H. and Shariff, A. M., 2016. An investigation of blended polymeric membranes and their gas separation performance. *RSC advances*, 6(104), pp.102671-102679.

Fila, K. Bolbukh, Y., Goliszek, M., Podkościelna, B., Gargol, M., and Gawdzik, B., 2019. Synthesis and characterization of mesoporous polymeric microspheres of methacrylic derivatives of aromatic thiols. *Adsorption*, Volume 25, pp.429-442.

Fu, J., Chen, Z., Wang, M., Liu, S., Zhang, J., Zhang, J., Han, R., and Xu, Q., 2015. Adsorption of methylene blue by a high-efficiency adsorbent (polydopamine microspheres): kinetics, isotherm, thermodynamics and mechanism analysis. *Chemical Engineering Journal*, Volume 259, pp.53-61.

Gonsalvesh, L., Marinov, S. P., Gryglewicz, G., Carleer, R., and Yperman, J., 2016. Preparation, characterization and application of polystyrene based activated carbons for Ni (II) removal from aqueous solution. *Fuel Processing Technology*, Volume 149, pp.75-85.

Guerrero-Pérez, M. O. and Patience, G. S., 2020. Experimental methods in chemical engineering: Fourier transform infrared spectroscopy—FTIR. *The Canadian Journal of Chemical Engineering*, 98(1), pp.25-33.

Guillen, G. R., Pan, Y., Li, M. and Hoek, E. M., 2011. Preparation and characterization of membranes formed by nonsolvent induced phase separation: a review. *Industrial & Engineering Chemistry Research*, 50(7), pp.3798-3817.

Gujar, R. B. and Mohapatra, P. K., 2015. Amazing selectivity for Am (III) uptake by composite graphene oxide-PES polymeric beads prepared by phase inversion. *RSC advances*, 5(31), pp.24705-24711.

Gupta, A., Sharma, V., Sharma, K., Kumar, V., Choudhary, S., Mankotia, P., Kumar, B., Mishra, H., Moulick, A., Ekielski, A., and Mishra, P. K., 2021. A review of adsorbents for heavy metal decontamination: Growing approach to wastewater treatment. *Materials*, 14(16), p.4702.

Han, M. G., Lee, Y. J., Byun, S. W. and Im, S. S., 2001. Physical properties and thermal transition of polyaniline film. *Synthetic Metals*, 124(2-3), pp.337-343.

Hellal, M. S., Rashad, A. M., Kadimpati, K. K., Attia, S. K., and Fawzy, M. E., 2023. Adsorption characteristics of nickel (II) from aqueous solutions by Zeolite Scony Mobile-5 (ZSM-5) incorporated in sodium alginate beads. *Scientific Reports*, 13(1), p.19601.

Hering, J. G., 2017. Managing the 'monitoring imperative' in the context of SDG target 6.3 on water quality and wastewater. *Sustainability*, 9(9), p.1572.

Hunter Lab, 2022. *What scale is used to measure the color of waste water?*. [Online]

Available at: <<https://support.hunterlab.com/hc/en-us/articles/201482339-What-scale-is-used-to-measure-the-color-of-waste-water>>

[Accessed 27 March 2024].

Jadoun, S., Fuentes, J. P., Urbano, B. F. and Yáñez, J., 2022. A review on adsorption of heavy metals from wastewater using conducting polymer-based materials. *Journal of Environmental Chemical Engineering*, p.109226.

- Jyothi, N. V. N., Prasanna, P. M., Sakarkar, S. N., Prabha, K. S., Ramaiah, P. S., and Srawan, G. Y., 2010. Microencapsulation techniques, factors influencing encapsulation efficiency. *Journal of microencapsulation*, 27(3), pp.187-197.
- Karimifard, S. and Moghaddam, M. R. A., 2018. Application of response surface methodology in physicochemical removal of dyes from wastewater: a critical review. *Science of the Total Environment*, Volume 640, pp.772-797.
- Khan, I., Saeed, K., Zekker, I., Zhang, B., Hendi, A. H., Ahmad, A., Ahmad, S., Zada, N., Ahmad, H., Shah, L. A., Shah, T., and Khan, I., 2022. Review on methylene blue: Its properties, uses, toxicity and photodegradation. *Water*, 14(2), p.242.
- Khan, S. A., Rehan, Z. A., Alharthi, S. S., Alosaimi, E. H., Gzara, L., El-Shahawi, M. S., Alamry, K. A., Akhtar, K., Bakhsh, E. M., Asiri, A. M., Khan, S. B., and Drioli, E., 2021. Polyethersulfone coated Ag-SiO₂ nanoparticles: a multifunctional and ultrafiltration membrane with improved performance. *Desalination and Water Treatment*, Volume 239, pp.217-227.
- Krishna, R. H., Chandraprabha, M. N., Samrat, K., Murthy, T. K., Manjunatha, C., and Kumar, S. G., 2023. Carbon nanotubes and graphene-based materials for adsorptive removal of metal ions—A review on surface functionalization and related adsorption mechanism. *Applied Surface Science Advances*, Volume 16, p.100431.
- Lakherwal, D., 2014. Adsorption of heavy metals: a review. *International journal of environmental research and development*, 4(1), pp.41-48.
- Lakshmi, D. S., Figoli, A., Buonomenna, M. G., Golemme, G., and Drioli, E., 2012. Preparation and characterization of porous and nonporous polymeric microspheres by the phase inversion process. *Advances in Polymer Technology*, 31(3), pp.231-241.
- Lee, J. and Patel, R., 2022. Wastewater treatment by polymeric microspheres: A review. *Polymers*, 14(9), p.1890.
- Mallakpour, S. and Rashidimoghadam, S., 2019. Microscopic characterization techniques for layered double hydroxide polymer nanocomposites. In: *Layered Double Hydroxide Polymer Nanocomposites*. s.l.:Woodhead Publishing, pp.157-203.
- Mashkoo, F., Nasar, A. and Inamuddin., 2020. Carbon nanotube-based adsorbents for the removal of dyes from waters: a review.. *Environmental Chemistry Letters*, 18(3), pp.605-629.
- Mehdi, S. U. and Aravamudan, K., 2022. Adsorption of cadmium ions on silica coated metal organic framework. *Materials Today: Proceedings*, Volume 61, pp.487-497.
- Mohamed, M. A., Jaafar, J., Ismail, A. F., Othman, M. H. D., and Rahman, M. A., 2017. Fourier transform infrared (FTIR) spectroscopy. *Membrane characterization*, pp.3-29.
- Moradihamedani, P., 2022. Recent advances in dye removal from wastewater by membrane technology: a review. *Polymer Bulletin*, 79(4), pp. 2603-2631.

- Nasrollahzadeh, M., Atarod, M., Sajjadi, M., Sajadi, S. M., and Issaabadi, Z., 2019. Plant-mediated green synthesis of nanostructures: mechanisms, characterization, and applications. In: *Interface science and technology*. s.l.:Elsevier, pp.199-322.
- Neolaka, Y. A., Riwu, A. A., Aigbe, U. O., Ukhurebor, K. E., Onyancha, R. B., Darmokoesoemo, H., and Kusuma, H. S., 2022. Potential of activated carbon from various sources as a low-cost adsorbent to remove heavy metals and synthetic dyes. *Results in Chemistry*, Volume 5, p.100711.
- Obaideen, K., Shehata, N., Sayed, E. T., Abdelkareem, M. A., Mahmoud, M. S., and Olabi, A. G., 2022. The role of wastewater treatment in achieving sustainable development goals (SDGs) and sustainability guideline. *Energy Nexus*, Volume 7, p.100112.
- Oladoye, P. O., Ajiboye, T. O., Omotola, E. O. and Oyewola, O. J., 2022. Methylene blue dye: Toxicity and potential elimination technology from wastewater. *Results in Engineering*, Volume 16, p. 100678.
- Peña, B., Panisello, C., Aresté, G., Garcia-Valls, R., and Gumí, T., 2012. Preparation and characterization of polysulfone microcapsules for perfume release. *Chemical Engineering Journal*, Volume 179, pp.394-403.
- Qasem, N. A., Mohammed, R. H. and Lawal, D. U., 2021. Removal of heavy metal ions from wastewater: a comprehensive and critical review. *Npj Clean Water*, 4(1), p.36.
- Rajendran, S., Priya, A. K., Kumar, P. S., Hoang, T. K., Sekar, K., Chong, K. Y., Khoo, K. S., Ng, H. S., Show, P. L., 2022. A critical and recent developments on adsorption technique for removal of heavy metals from wastewater-A review. *Chemosphere*, Issue 135146, p.303.
- Rajisha, K. R., Deepa, B., Pothan, L. A. and Thomas, S., 2011. Thermomechanical and spectroscopic characterization of natural fibre composites. *Interface engineering of natural fibre composites for maximum performance*, pp.241-274.
- Rápó, E. and Tonk, S., 2021. Factors affecting synthetic dye adsorption; desorption studies: a review of results from the last five years (2017–2021). *Molecules*, 26(17), p.5419.
- Renu, Agarwal, M. and Singh, K., 2017. Heavy metal removal from wastewater using various adsorbents: a review. *Journal of Water Reuse and Desalination*, 7(4), pp.387-419.
- Rozaini, C. A., Jain, K., Oo, C. W., Tan, K. W., Tan, L. S., Azraa, A., and Tong, K. S., 2010. Optimization of nickel and copper ions removal by modified mangrove barks. *International Journal of Chemical Engineering and Applications*, 1(1), p.84.
- Sahu, O. P. and Chaudhari, P. K., 2013. Review on chemical treatment of industrial waste water. *Journal of Applied Sciences and Environmental Management*, 17(2), pp.241-257.

Sandoval-Olvera, I. G., Villafana-Lopez, L., Reyes-Aguilera, J. A., Ávila-Rodríguez, M., Razo-Lazcano, T. A., and González-Muñoz, M. P., 2017. Surface modification of polyethersulfone membranes with goethite through self-assembly. *Desalin. Water Treat*, Volume 65, pp.199-207.

Scimeca, M., Bischetti, S., Lamsira, H. K., Bonfiglio, R., and Bonanno, E., 2018. Energy Dispersive X-ray (EDX) microanalysis: A powerful tool in biomedical research and diagnosis. *European journal of histochemistry: EJH*, 62(1).

Shi, H., Dong, C., Yang, Y., Han, Y., Wang, F., Wang, C., and Men, J., 2020. Preparation of sulfonate chitosan microspheres and study on its adsorption properties for methylene blue. *International Journal of Biological Macromolecules*, Volume 163, pp.2334-2345.

Shi, J., Teng, X., Suo, Q., Mojiri, A., Taghavijeloudar, M., and Rezania, S., 2023. Novel magnetic polyethersulfone-polyethyleneimine-based microbeads for removal of lead ions from water: Kinetics and thermodynamics. *Journal of Molecular Liquids*, Volume 387, p.122632.

Soliman, N. K. and Moustafa, A. F., 2020. Industrial solid waste for heavy metals adsorption features and challenges; a review. *Journal of Materials Research and Technology*, 9(5), pp.10235-10253.

Sopyan, I. Y. A. N., Gozali, D. O. L. I. H. and Guntina, R. K., 2022. Design-expert software (DOE): An application tool for optimization in pharmaceutical preparations formulation. *Int. J. Appl. Pharm*, 14(4), pp.55-63.

Sulejmanović, J., Memić, M., Šehović, E., Omanović, R., Begić, S., Pazalja, M., Ajanović, A., Azhar O., Sher, F., 2022. Synthesis of green nano sorbents for simultaneous preconcentration and recovery of heavy metals from water. *Chemosphere*, Volume 296, p.133971.

Tan, W. Y., Shuit, S. H., Lim, S., Tee, S. F., Pang, Y. L., and Ng, Q. H., 2023. Development of high reusability trifunctional polyethersulfones microspheres for the removal of methyl orange. *Journal of Water Process Engineering*, Volume 51, p.103347.

Tkachenko, Y. and Niedzielski, P., 2022. FTIR as a method for qualitative assessment of solid samples in geochemical research: A review. *Molecules*, 27(24), p.8846.

Upadhyay, U., Sreedhar, I., Singh, S. A., Patel, C. M., and Anitha, K. L., 2021. Recent advances in heavy metal removal by chitosan based adsorbents. *Carbohydrate Polymers*, Volume 251, p.117000.

US Department of Health, 2022. *Arsenic in Drinking Water*. [Online] Available at: <<https://www.health.state.mn.us/communities/environment/water/contaminant/s/arsenic.html>> [Accessed 12 July 2023].

Varghese, A. G., Paul, S. A. and Latha, M. S., 2019. Remediation of heavy metals and dyes from wastewater using cellulose-based adsorbents. *Environmental Chemistry Letters*, Volume 17, pp.867-877.

Wang, H. H., Jung, J. T., Kim, J. F., Kim, S., Drioli, E., and Lee, Y. M., 2019. A novel green solvent alternative for polymeric membrane preparation via nonsolvent-induced phase separation (NIPS). *Journal of membrane science*, Volume 574, pp.44-54.

Wasif, M., Sarfraz, M., Tahir, Z., and Nawaz, S., 2023. Pursuit of high-performance carbon capture membranes: fabrication of nickel oxide-doped polyethersulfone-based mixed matrix membranes. *Polymer Bulletin*, pp.1-14.

Xia, Y., Yao, Q., Zhang, W., Zhang, Y., and Zhao, M., 2019. Comparative adsorption of methylene blue by magnetic baker's yeast and EDTAD-modified magnetic baker's yeast: equilibrium and kinetic study. *Arabian Journal of Chemistry*, 12(8), pp.2448-2456.

Yadav, M., Singh, G. and Jadeja, R. N., 2021. Physical and chemical methods for heavy metal removal. *Pollutants and Water Management: Resources, Strategies and Scarcity*, pp.377-397.

Yang, K., Liu, J., Li, S., Li, Q., Wu, Q., Zhou, Y., Zhao, Q., Deng, N., Liang, Z., Zhang, L., and Zhang, Y., 2014. Epitope imprinted polyethersulfone beads by self-assembly for target protein capture from the plasma proteome. *Chemical communications*, 50(67), pp.9521-9524.

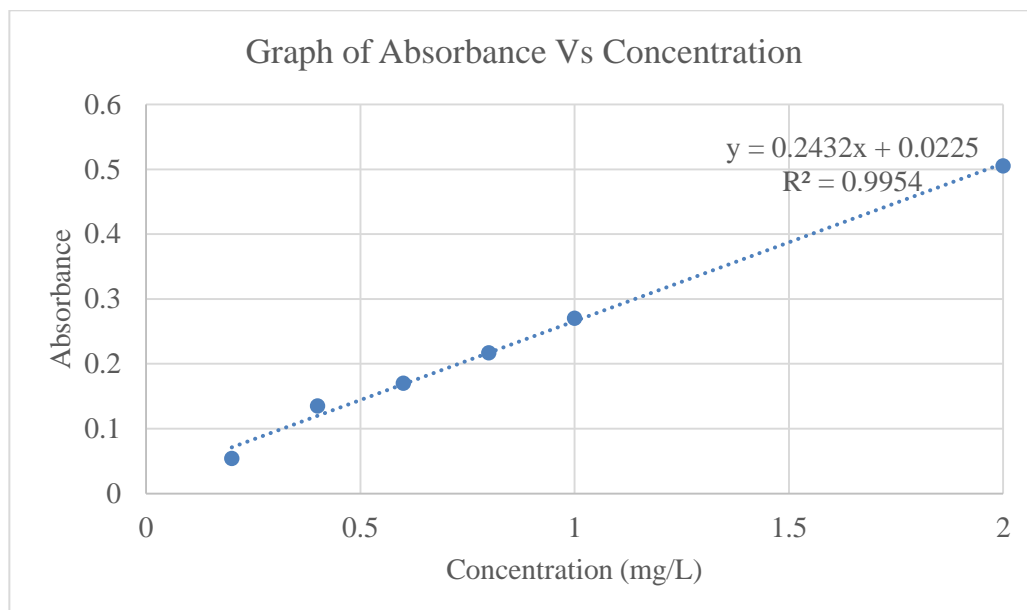
Yao, T., Guo, S., Zeng, C., Wang, C., and Zhang, L., 2015. Investigation on efficient adsorption of cationic dyes on porous magnetic polyacrylamide microspheres. *Journal of hazardous materials*, Volume 292, pp.90-97.

Yee, L. Y., Ng, Q. H., Shuit, S. H., Enche Ab Rahim, S. K., Mohammad Nawi, D., and Low, S. C., 2021. Application of the novel pH-catalytic-magnetic tri-functionalities augmented bead for removal of organic dye pollutants. *Environmental Progress and Sustainable Energy*, 40(6), p.e13699.

Zaynab, M., Al-Yahyai, R., Ameen, A., Sharif, Y., Ali, L., Fatima, M., Khan, K. A., and Li, S., 2022. Health and environmental effects of heavy metals. *Journal of King Saud University-Science*, 34(1), p.101653.

Zhang, S., Dai, F., Wang, Q., Qian, G., Chen, C., and Yu, Y., 2022. The fabrication of porous hollow polysulfone microspheres with PEG as a porogen for methylene blue adsorption. *Colloids and Surfaces A: Physicochemical and Engineering Aspects*, Volume 634, p.127949.

Zhu, H., Chen, S. and Luo, Y., 2023. Adsorption mechanisms of hydrogels for heavy metal and organic dyes removal: A short review. *Journal of Agriculture and Food Research*, Volume 12, p.100552.

APPENDICES**Appendix A: Standard Calibration Curve of Methylene Blue****Graph A-1: Calibration Curve of Methylene Blue Solution**